Rational Design of Novel, Potent Small Molecule Pan-Selectin Antagonists

Remo Kranich, Anke S. Busemann, Daniel Bock, Sabine Schroeter-Maas, Diana Beyer, Bo Heinemann, Michael Meyer, Katrin Schierhorn, Rainer Zahlten, Gerhard Wolff, and Ewald M. Aydt*

Revotar Biopharmaceuticals AG, Neuendorfstrasse 24a, 16761 Hennigsdorf, Germany

Received May 9, 2006

This report describes the first results of a rational hit-finding strategy to design novel small molecule antiinflammatory drugs targeting selectins, a family of three cellular adhesion molecules. Based on recent progress in understanding of molecular interaction between selectins and their natural ligands as well as progress in clinical development of synthetic antagonists like **1** (bimosiamose, TBC1269), this study was initiated to discover small molecule selectin antagonists with improved pharmacological properties. Considering **1** as template structure, a ligand-based approach followed by focused chemical synthesis has been applied to yield novel synthetic small molecules ($MW_r < 500$) with a trihydroxybenzene motif, bearing neither peptidic nor glycosidic components, with nanomolar *in vitro* activity. Biological evaluation involves two kinds of *in vitro* assays, a static molecular binding assay, and a dynamic HL-60 cell attachment assay. As compared to controls, the novel compounds showed improved biological *in vitro* activity both under static and dynamic conditions.

Introduction

Transmigration of leukocytes (e.g., monocytes, lymphocytes, eosinophils, neutrophils, and basophils) from the circulation into the surrounding tissue is of vital importance to maintain innate and adaptive immune defense mechanisms under physiological conditions and pathological stages like injury or inflammatory response. This multistep process is governed by a coordinated interplay involving a broad spectrum of adhesion and signaling molecules.[1] Different from this highly regulated cascade, dysregulation of leukocyte transmigration results in uncontrolled excessive and pathological infiltration of leukocytes into organs. Finally, it leads to acute and chronic inflammatory diseases such as acute lung injury (ALI), acute respiratory distress syndrome (ARDS), asthma, chronic obstructive pulmonary diseases (COPD), psoriasis, and rheumatoid arthritis. Therefore, adhesion and signaling molecules are an attractive target to develop novel drugs for the treatment of acute and chronic inflammatory diseases.

The first step in transmigration is mediated by the selectin family of cell adhesion molecules, which consists of three structurally related calcium-dependent carbohydrate binding proteins, E-, P-, and L-selectin.[2] P-selectin is a rapidly inducible selectin found only on activated platelets and vascular endothelium. E-selectin is an intermediate inducible selectin found primarily on activated vascular endothelial cells. L-selectin is constitutively expressed on the surface of several leukocyte subtypes, including neutrophils, monocytes, the majority of circulating B- and T-cells, and on a subset of natural killer cells. Physiologically, selectins mediate the initial rolling or tethering of leukocytes on the vascular endothelium to allow them to adhere to the vascular endothelium and, consequently, to initiate transmigration from the vascular circulation into the surrounding tissue. Under pathological conditions, however, e.g., local or systemic inflammation and/or injury of the vascular system, this fundamental process is up-regulated, at least in part, due to an increase in the expression of E- and P-selectin. The process of leukocyte rolling is generally considered to be a primary event in the inflammatory response and thus constitutes an attractive target for therapeutic intervention.

For the interaction between selectins and their natural ligands, the tetrasaccharide sialyl Lewis^X (sLe^X, [Neu5Acα2-3Galβ1−4(Fucα1−3)GlcNAc], **2**, Figure 1), and related oligosaccharides have been identified as key functional groups.[3] SLe^X which binds with low affinity to E-, P-, and L-selectin was found to be a common epitope in many natural selectin ligands, such as P-selectin glycoprotein ligand 1 (PSGL-1), glycosylated cell adhesion molecule 1 (GlyCAM-1), CD34, mucosal addressin cell adhesion molecule 1 (MAdCAM-1), and E-selectin ligand 1 (ESL-1).[4] The identification of this epitope and its importance has guided the design of selectin inhibitors in the past. Thus, efforts to develop novel selectin antagonists have been mainly focused on the design of sLe^X glycomimetics, glycosylated peptides, or peptides.[5] Since many natural high affinity ligands provide multivalent arrangement of binding epitopes to selectins, one approach to overcome the low affinity of monomeric sLe^X-mimetics is multivalent assembly of sLe^X-mimetics.[6] However, these compounds may suffer from several problems regarding development as pharmaceutical agents. As compared to the large number of reports on glycosidic and peptidic sLe^X-mimetics, only few reports on nonglycosylated and nonpeptidic selectin antagonists are published.[7−9] In this regard, several excellent reviews were published summarizing the history and current activities in the field of selectin antagonists.[10−11]

To date, almost all efforts to design novel therapeutically effective sLe^X-mimicking selectin antagonists failed, which is supposed to be caused by different reasons.[12] First, many selectin antagonists effectively inhibit only one or two of the three selectins. However, there is functional redundancy between selectins, e.g., between E- and P-selectin on the vascular endothelial surface, allowing to bypass inhibition of single-type selectin family members.[13] Second, there is only a weak interaction between selectins and sLe^X implying K_Ds in the mM range for P- and L-selectin and in the higher μM range for E-selectin.[14] Thus, novel compounds designed on the basis of sLe^X only are likely to be a selectin antagonists with high K_D values. Third, sLe^X and structurally related low affinity ligands failed to inhibit P- and L-selectin mediated rolling *in vivo*.

* To whom correspondence should be addressed. E-mail: e.aydt@revotar-ag.de. Tel: +49 (0)3302 202 5069. Fax: +49 (0)3302 202 5030.

10.1021/jm060536g CCC: $37.00
Published on Web 02/16/2007

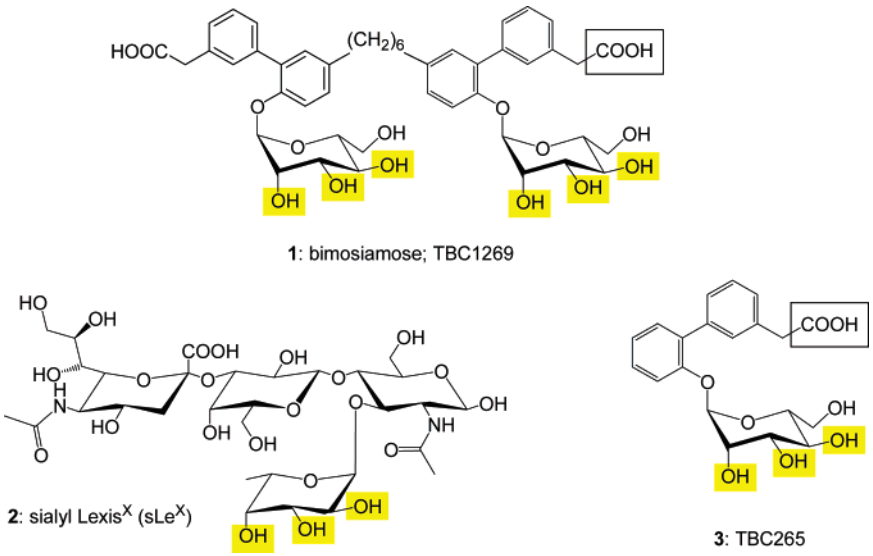

Figure 1. Structure of **1** (bimosiamose, TBC1269), a dimer-like (α-D-Mannopyranosyloxy)biphenyl-substituted carboxylic acid. Sialyl Lexis^X (**2**) is itself a natural low affinity ligand of selectins as well as a crucial binding moiety of many natural ligands of selectins, such as the high affinity P-selectin glycoprotein ligand 1 (PSGL-1). Structure of **3** (TBC265), a substructure of **1**, and first generation lead structure in the development of **1**. Stereochemically equivalent hydroxyls at C-2, C-3, and C-4 of mannose in **1** or **3** and C-4, C-3, and C-2 of fucose in sLe^X are highlighted. The boxes around the carboxylic acids in compound **1** and **3** indicate potentially crucial groups for competing with tyrosine-sulfate-51 in PSGL-1. Note that in compound **1** only one of two carboxylic acids is marked. SAR studies showed that only one carboxylic acid in compound **1** is required for activity.[23]

E-selectin-mediated *in vivo* rolling is only influenced at high doses.[15] High affinity of natural selectin ligands is supposed to be, at least in part, due to multivalent arrangement of binding epitopes as well as extensive surface contacts between selectins and their ligands.[16] Recently, for instance, the nature of the high affinity binding of a glycoprotein-type ligand and P-selectin has been solved in atomic detail. P-selectin glycoprotein ligand 1 (PSGL-1) binds with nanomolar *in vitro* activity to P-selectin, but it also binds to E- and L-selectin. It was shown by biochemical and structural investigations that sulfated tyrosine residues are in addition to the occurrence of sLe^X mandatory for high affinity binding to P-selectin.[17] Even though the interaction between PSGL-1 and P-selectin comprises a large surface area, the close proximity between essential binding features offers the opportunity for the design of selectin antagonists that compete with PSGL-1 and PSGL-1-like ligands for selectin binding.

Using PSGL-1 as major high affinity template structure, a rational drug design approach to discover novel potent synthetic nonglycosidic and nonpeptidic small molecule pan-selectin antagonists is presented. Based on **1** (bimosiamose, TBC1269, Figure 1), a ligand-based design strategy followed by focused chemical synthesis was applied. *In silico* considerations led to synthetic polyphenolic small molecules with $MW_r < 500$ and nanomolar *in vitro* activity in the static molecular binding assay. In this assay synthetic antagonists compete with a PSGL-1-like ligand for selectin binding. In addition, the compounds inhibit the *in vitro* attachment of HL-60 cells to E- and P-selectin matrices. To our knowledge, this is the first time that synthetic small molecules $MW_r < 500$ and yet with nanomolar *in vitro* activity are reported.

Rational Drug Design

The structure of E- and P-selectin has been solved in atomic detail.[18,19] In addition, cocrystals of P-selectin with sLe^X and PSGL-1 as well as cocrystals of E- selectin with sLe^X have been solved.[19] A structure-based approach in order to search for new selectin antagonists seems therefore to be appropriate. However, the selectins belong to a class of molecules which are not readily amenable to receptor- or structure-based drug design for virtual screening even if the 3-D structure is available. This is due to structural characteristics of the ligand-binding site, which is an almost flat binding surface. Most docking algorithms work well for receptors or enzymes with more or less deep cavities providing spatial restraints to small molecule ligands, but due to the large number of degrees of freedom, shallow surfaces still represent a challenge for many docking algorithms. The applicability of an automated docking procedure to search for novel scaffolds was investigated in this study. The results of this analysis indicate that applying automated docking, as implemented in MOE,[20] is not applicable to quickly identify novel chemical scaffolds in the hit-finding process.

Therefore, a ligand-based approach has been employed being based on **1**, a selectin antagonist that was tested in Phase I and Phase IIa trials for the treatment of asthma and psoriasis.[21−22] Presently, further preclinical and clinical studies are ongoing. The molecule was identified as the most advanced pharmaceutical compound in the field of selectin antagonists,[10] and it appears to be an appropriate template for a ligand-based drug design. This approach resulted in a concept for a possible pharmacophore, followed by focused chemical synthesis.

The pan-selectin antagonist **1** has been rationally designed by Kogan et al. as sLe^X (**2**) mimetic.[23] It is a dimer type (α-D-mannopyranosyloxy)biphenyl-substituted carboxylic acid with $MW_r = 862.9$. As compared to the natural ligand sLe^X, **1** showed improved *in vitro* potency. Due to the fact, except for compound **1**, that none of the former reported drug discovery programs for the development of novel small molecule sLe^X mimetics succeeded in providing novel chemical entities with clinical efficacy, it was suggested that **1** might bind, at least in part, differently to selectins as compared to sLe^X. Molecular alignments of compound **3** (TBC265, Figure 1), a substructure of **1**, with sLe^X as well as comprehensive retrospective docking investigations of compound **1** on P-selectin revealed that **1** may mimic both sLe^X-specific binding features and a crucial molecular binding feature being specific for the N-terminal peptidic

Table 1. Biological *in Vitro* Data

	IC_{50} [μM] or % inhibition at 100 μM[a]			% inhibition HL-60 attachment[e]	
compound	E-selectin	P-selectin	L-selectin	E-selectin	P-selectin
1 (bimosiamose)	>500[b]	95.0	>500[b]	28	50
2 (sLe^X)[c]	134.2	>4000[d]	>4000[d]	32	n.s.[f]
3 (TBC265)	>500[b]	>500[b]	>500[b]	34	n.s.[f]
4	8.3%	1.7%	13.5%	47	24
5	>500[b]	19.1	27.6	n.s.[f]	n.s.[f]
6	19.5%	−16.1%	1.3%	n.a.[g]	n.a.[g]
7	31.7	31.8	38.5	n.a.[g]	n.a.[g]
8	>500[b]	11.8	15.2	n.a.[g]	n.a.[g]
9	6.0%	−3.0%	1.1%	n.a.[g]	n.a.[g]
10	25.6%	-1.0%	12.2%	n.a.[g]	n.a.[g]
11	37.6%	52.0%	51.7%	n.a.[g]	n.a.[g]
12	15.0%	−5.3%	4.3%	n.a.[g]	n.a.[g]
13	3.1%	77.0%	83.6%	n.a.[g]	n.a.[g]
14	>500[b]	0.87	1.5	16	35
29a	4.9	4.2	8.7	18	22
29b	85.4	43.2	64.9	20	22
34	>500[b]	57.2	154.4	29	n.s.[f]
35a	0.8	1.1	1.4	n.s.[f]	n.s.[f]
35b	18.7	19.6	46.6	n.s.[f]	n.s.[f]
36a	1.0	2.1	>500[b]	27	n.s.[f]
36b	2.3	2.3	2.3	19	n.s.[f]
38a	3.3	2.4	3.1	35	11
38b	41.9	10.2	13.6	35	11
39a	3.0	2.8	3.3	n.s.[f]	15
39b	3.1	3.4	5.7	n.s.[f]	n.s.[f]
40a	8.7	14.8	26.2	16	20
40b	8.4	34.9	30.8	21	21
41a	>500[b]	42.8	64.5	22	24
41b	1.3	2.9	4.2	n.s.[f]	17
42a	n.a.[g]	>500[b]	>500[b]	19	n.s.[f]
42b	8.4	21.7	109	n.s.[f]	n.s.[f]
44	>500[b]	7.6	14.6	26	n.s.[f]
46	52.4	53.9	105.1	n.s.[f]	n.s.[f]
48	>500[b]	24.8	41.7	26	47
50	>500[b]	28.6	85.8	n.s.[f]	n.s.[f]
52	48.6	19.5	21.3	28	23
54	57.2	3.4	4.3	n.s.[f]	56
56	132.0	5.8	9.8	61	55
58	>500[b]	21.8	37.6	32	45
60	113.7	212.1	244.0	n.s.[f]	25
61	61.4	1.2	1.6	53	98
62	9.7	0.57	0.79	47	83
63	48.0	1.1	1.6	33	58
64	15.7	0.74	1.1	58	93
65	>500[b]	3.6	9.7	n.s.[f]	58

[a] IC_{50} [μM] values are given for the static molecular binding assay for E-, P-, and L-selectin. Maximal tested concentration is 500 μM. If IC_{50}s are not available, %-inhibition at an inhibitor concentration of 100 μM will be given. [b] No IC_{50} value determinable up to a concentration of 500 μM. [c] SLe^X has been tested up to a concentration of 4000 μM. [d] No IC_{50} value determinable up to a concentration of 4000 μM. [e] %-inhibition of HL-60 cell attachment is given. Inhibitor concentration was 109 μM. [f] Not significant. [g] Not available.

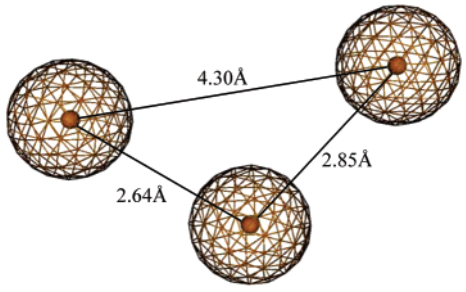

Figure 2. Early pharmacophoric model used for 3-D database searches. The pharmacophore represents an abstraction of three hydroxyl groups which are considered to be important for binding to selectins and can be found in the calcium binding sugars mannose, fucose, and arabinose. Each sphere represents a hydrogen bond acceptor and donator. Distances between the centers are 2.64 Å, 2.85 Å, and 4.30 Å. The tolerance radius was set to 0.8 Å.

fraction of PSGL-1.[24] According to the cocrystals of sLe^X and sLe^X-bearing PSGL-1 with P-selectin, the hydroxyl groups of fucose at C-4, C-3, and C-2 are involved in calcium binding and/or hydrogen bonding to P-selectin. Considering the equivalent stereochemical arrangement of hydroxyl groups at C-2, C-3, and C-4 of mannose in compound **1** or **3** and at C-4, C-3, and C-2 of fucose in sLe^X, it can be assumed that the mannosyl unit binds to the calcium ion on the surface of selectins in a similar manner as the fucosyl unit of sLe^X does (Figure 1). The stereochemical pattern of hydroxyl groups is also reflected by other selectin antagonists taking advantage of arabinose instead of fucose, further supporting the meaning of a common pharmacophore.[25] In addition, the docking investigations indicate that one of the carboxylic acid groups of **1** is likely to mimic the function of tyrosine sulfate-51 (Tys 51) of PSGL-1, another hot spot of the high affinity ligand PSGL-1, which in turn binds to Arg-85 of P-selectin.[19] In conclusion, hot spots mandatory for high affinity binding of PSGL-1 to P-selectin can also be found in **1**. Therefore, compound **1** can be considered as PSGL-1-glycopeptido-mimetic rather than sLe^X glyco-mimetic, whereby one of the mannosyl groups of **1** is supposed to bind to calcium and one of the carboxylic acids to Arg-85 of P-selectin. This

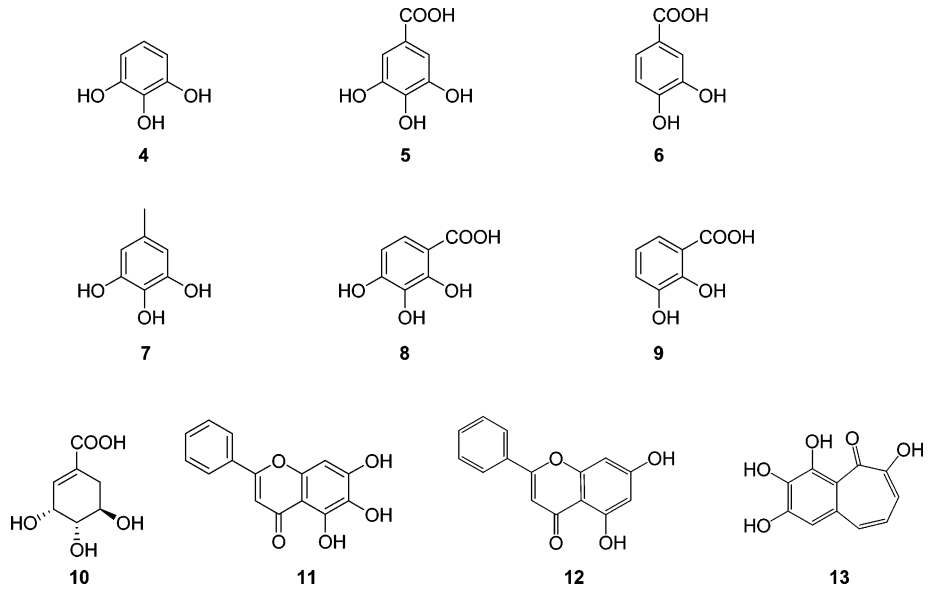

Figure 3. Selected hits of the *in silico* search procedure.

hypothesis is in agreement with biological *in vitro* experiments, where **1** potently competes with a PSGL-1-like ligand for P-selectin binding (Table 1).

On the basis of these findings, compound **1** is regarded as the template structure for a ligand-based design of novel nonpeptidic and nonglycosidic small molecule selectin antagonists with improved pharmacodynamic and pharmacokinetic properties. Due to its large number of rotatable bonds, compound **1** is, however, not the best starting point for a ligand-based design approach. Interestingly, Kogan et al. showed that only one of the two carboxylic groups in compound **1** is mandatory for selectin binding, indicating that both structurally identical subunits of **1** may contribute differently to selectin binding.[23] Therefore, compound **3**, a substructure of **1** and historically the first generation lead structure in the development of **1** was taken as a starting structure.[26] This substructure is basically half of **1** and, like **1**, is supposed to interfere with not only the sLe^X binding feature but also a peptidic binding feature of PSGL-1. Although **3** did not show inhibitory activity in the PSGL-1-like setting (static molecular binding assay) at given concentrations (Table 1), the compound showed activity in another *in vitro* selectin assay at higher concentration and can therefore be considered as a weak binder.[26] As already mentioned above, the hydroxyl groups at C-2, C-3, and C-4 of mannose in **3**, which are likely to reflect the function of the hydroxyl groups at C-4, C-3, and C-2 of fucose in sLe^X, are supposed to be crucial for selectin binding. In the case of sLe^X, two of the fucosyl hydroxyls bind to calcium on the shallow surface of the C-type lectin domain of selectins.[19] All three hydroxyl groups participate in hydrogen bonding to selectins. Furthermore, the carboxylic acid group of **3**, which is supposed to mimic Tys 51 of PSGL-1, is also considered to be crucial for selectin binding.

Taking compound **3** as the new template, initial efforts were focused on the replacement of the mannose moiety. The three-dimensional structure of **3** was minimized by employing a stochastic search algorithm and the MMFF94x force field. From the position of hydroxyls at C-2, C-3, and C-4 of mannose, a pharmacophore was derived (Figure 2). In order to analyze conformational differences between the positions of the hydroxyl groups in the minimized mannose and the corresponding hydroxyl groups of the fucosyl unit in sLe^X as solved by crystallography,[19] a rigid superposition of the three hydroxyl groups of the minimized mannose of compound **3** with fucose was employed. The root-mean-square distance (rmsd) of 0.098 Å clearly demonstrates the structural equivalence of the hydroxyl groups and confirms validity of the energy minimization of compound **3** in a protein-free state. Accordingly, a 3-D database search against vendor databases was performed in order to identify molecular fragments appropriate for the replacement of mannose, which resulted in a large number of *in silico* hits. The hit set was then reduced by manual inspection whereby main criteria for exclusion were (1) molecular weight of the molecule, (2) no potential for chemical modifications, and (3) a peptidic and glycosidic nature of the molecular fragments. The resulting compounds were then acquired and tested in our *in vitro* assays. Examples from this exercise are shown in Figure 3. Both compounds **4** (pyrogallol) and **5** (gallic acid) showed *in vitro* inhibitory activity for P- and L-selectin in the static molecular binding assay with IC_{50} values in the lower μM range. Compound **4**, but not **5**, also showed activity in the dynamic HL-60 cell attachment assay. Compound **8,** a regioisomer of **5**, showed IC_{50} values comparable to that of **5**. Removing one of the hydroxyls of **5** or **8** resulted in compounds **6** and **9**, respectively, which were devoid of inhibitory effect for P- and L-selectin. However, inhibition of E-selectin was increased by both **6** and **9**. Calcium binding and hydrogen bonding of the hydroxyls were assumed, but electronic effects (e.g., π-bonding), or a combination of both might be possible as well. Further structure−activity relationship (SAR) studies are required and are part of ongoing research activities.

Other *in silico* hits, such as **10** (shikimic acid), which is known to bind to C-type lectin MBP-A,[27] as well as salicylates (not shown here), have also been investigated for their inhibitory action but with moderate activity in the static molecular binding assay. Interestingly, Kaila et al. recently reported on novel selectin antagonists. The authors describe quinic acid-derived compounds, a biochemical precursor of compound **10**, which was developed through structure-based design.[9] The authors applied a fragment-based design approach to identify molecular entities with moderate activity. Selected synthetic quinic acid derivatives showed promising biological activity both *in vitro* and *in vivo*. Two further *in silico* hit compounds, **11** (Baicalein) and **12** (Chrysin), also showed moderate biological *in vitro* activity. Compound **11** (5,6,7-trihydroxyflavone) is one of the three major flavonoids of *Scutellaria baicalensis* Georgi, a traditional Chinese herb with known antiinflammatory activity.[28]

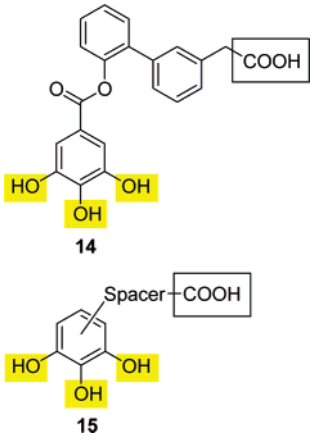

Figure 4. Hit compound **14** represents the gallic acid analogue of **3**. Presumably crucial binding motifs are highlighted. Motif **15** represents a generic structure for the compounds described in the following.

Compound **12** (5,7-dihydroxyflavone) belongs to the class of isoflavones with various biological activities.[29] Both compounds showed activity in the static molecular binding assay in the intermediate μM range. Actually, flavonoids are well-known as compounds with antiinflammatory effect[30] and have been described as selectin antagonists.[31] Finally compound **13** showed inhibitory activity against P- and L-selectin.

Taking synthetic aspects and the screening results of Table 1 into account, compound **5** seem to be the most appropriate replacement for mannose in **3**. Compound **10** has also been further investigated as a substitute for mannose but without success (data not shown). Substitution of mannose in **3** with **5** led to compound **14** (Figure 4), a gallic acid analogue of **3**. This compound proved to have IC_{50} values for P- and L-selectin in the high nM range and low μM range (see Table 1), respectively. However, compound **14** did not show inhibitory activity for E-selectin up to a concentration of 500 μM. Compound **14** has also been investigated in the dynamic HL-60 cell attachment assay and inhibited cell attachment to E- (16%) and P-selectin (35%), with inhibition rates below the values of the reference compound **1** (E: 28%; P: 50%). Furthermore, compound **14** can easily be aligned with compound **3** (Figure 5). After having found a new chemical scaffold by applying a ligand-based approach, a focused diversity approach followed. Here, a series of compounds with the general structure **15** (Figure 4) were synthesized and assayed for their biological activity. The intention of this procedure was to discover selectin antagonists with improved *in vitro* activity belonging to the structural space of **15**.

Chemistry

The first objective of this approach was to synthesize compound **14**, a gallic acid analogue of **3.** Thus a synthetic route analogous to the preparation of **3** was pursued (Scheme 1), whereby a compatible orthogonal protecting group strategy had to be applied to obtain **14**. The first challenge at this stage was to avoid the cleavage of the ester bond between the biphenyl and the gallic acid moiety throughout the reaction sequence. Due to the sensitivity of this ester bond against strong basic and acidic reaction conditions, the carboxylic acid function on the biphenyl moiety was protected as benzyl ester which could be cleaved afterward by hydrogenation. The hydroxyls of the gallic acid subunit were acetylated before the coupling step and could be cleaved later on under mild basic conditions (aqueous ammonia).

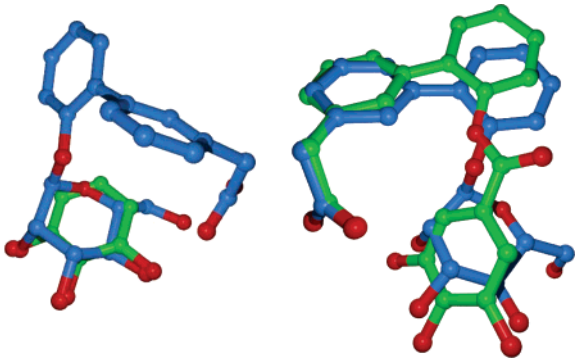

Figure 5. On the left-hand side molecule **4** (pyrogallol; carbon atoms in green) is aligned with a minimized structure of **3** (TBC265; carbon atoms in blue). The spatial correspondence of oxygens (red) is evident. On the right-hand side the best scoring superposition of **14** (carbon atoms in green) and **3** (carbon atoms in blue) is depicted. A flexible alignment procedure was applied with equally weighted similarity terms for hydrogen-bond donators and acceptors, aromaticity, acid/base, and volume, as implemented in MOE.[20] The structure of mannose in **3** was kept fixed in a minimized conformation. All other structural elements in compound **3** and **14** were flexible. Hydrogen atoms are omitted from the structures for clearance.

Esterification of 3-bromophenylacetic acid with benzyl bromide and $NaHCO_3$ delivered the first building block (**17**). THP[a1] protection of phenol with 3,4-DHP and PPTS followed by selective ortho-boration with *n*-BuLi and tri-isopropyl borate provided the second building block (**18**). Suzuki coupling of **17** and **18** with $Pd(PPh_3)_4$ to generate related orthogonally protected biphenyl **19** and release of phenolic hydroxyl under acidic conditions (*p*-TsOH, MeOH) led to **20**. Subsequent reaction with 5-(chlorocarbonyl)benzene-1,2,3-triyl triacetate (**21**) and final cleavage of acetyl groups of **22** with aqueous ammonia followed by Pd/C-catalyzed hydrogenation gave **14**.

Initially, molecule **14** was modified to investigate the effect of $-CH_2-$ and $-CH_2CH_2-$ spacer between the pyrogallol moiety and the carboxylic acid part of the molecule. Additionally, the ester function between the biphenyl and the gallic acid was replaced with an amide bond to facilitate chemical accessibility of the target molecules and to enhance the compatibility with a variety of reaction conditions (as well as with *in vitro*/*in vivo* conditions for later assays) leading to derivatives outlined in Scheme 2. Suzuki reaction of 3-bromophenylacetic acid methyl ester (**24**) with 2-aminophenylboronic acid hydrochloride in the presence of $Pd(PPh_3)_4$ under basic aqueous conditions provided desired biphenyl **25**. Amides **27** were then obtained by EDC coupling of compound **25** and 3,4,5-trimethoxyphenyl acetic (**26a**) or propionic acid (**26b**). Carboxylic acids **29** were subsequently prepared from **27** either by direct demethylation with BBr_3 (**29a**) or by analogue demethylation of the saponified intermediate **28** (LiOH in MeOH) leading to **29b**.

Next, γ-aminobutyric acid (GABA) was chosen as a spacer to further expand the distance between the carboxylic acid and pyrogallol portion of the molecule. As shown in Scheme 3, γ-amino butyric acid ethyl ester was treated with 3,4,5-trimethoxybenzoic acid chloride followed by ester hydrolysis with aqueous LiOH resulting in building block **31**. Following an analogous sequence as described above, EDC coupling of

[a] Abbreviations: THP, tetrahydropyranyl; DHP, dihydro-*2H*-pyran; PPTS, pyridinium *p*-toluenesulfonate; EDC, 1-(3-dimethylaminopropyl)-3-ethylcarbodiimide; DMAP, 4-*N*,*N*′-dimethylaminopyridine; DIC, diisopropylcarbodiimide; Pd/C, palladium on carbon (10% w/w); rt, room temperature; aq, aqueous, t_R, retention time; MW_r, relative molecular weight.

Scheme 1. Synthesis of TBC265 (**3**)-Analogous Compound **14**

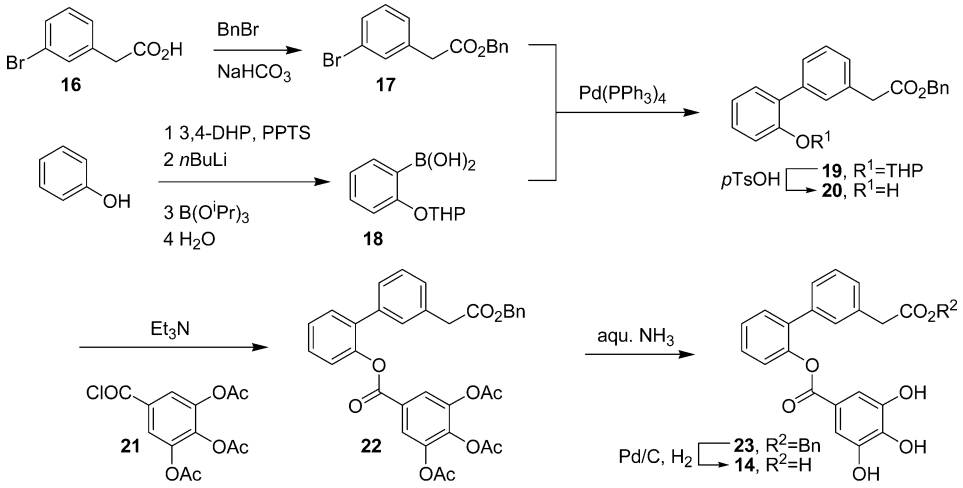

Scheme 2. Synthesis of Homologous Compounds **29** via Biphenyl **25**[a]

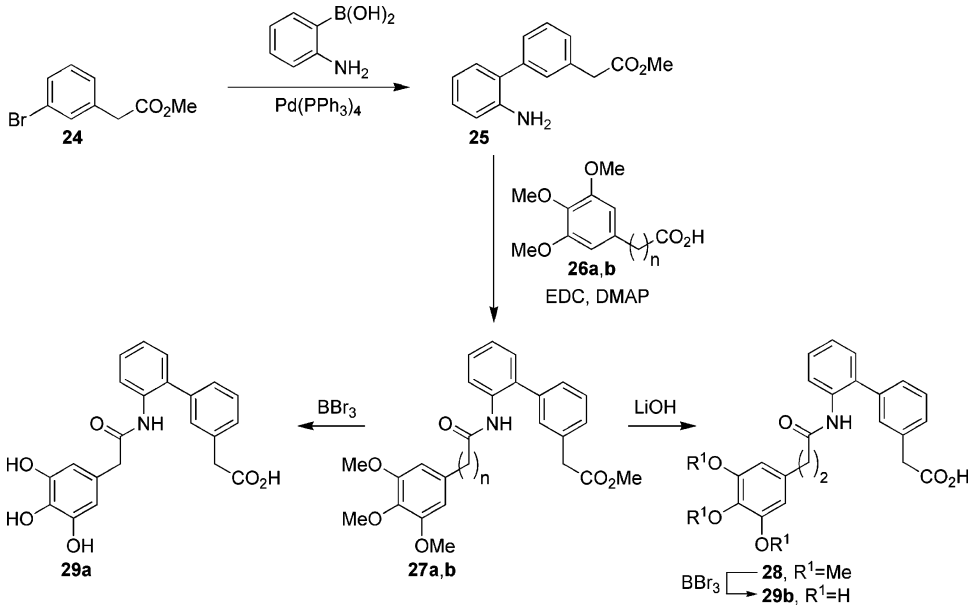

[a] For **a**, $n = 1$ and **b** $n = 2$.

Scheme 3. Synthetic Route to **34**

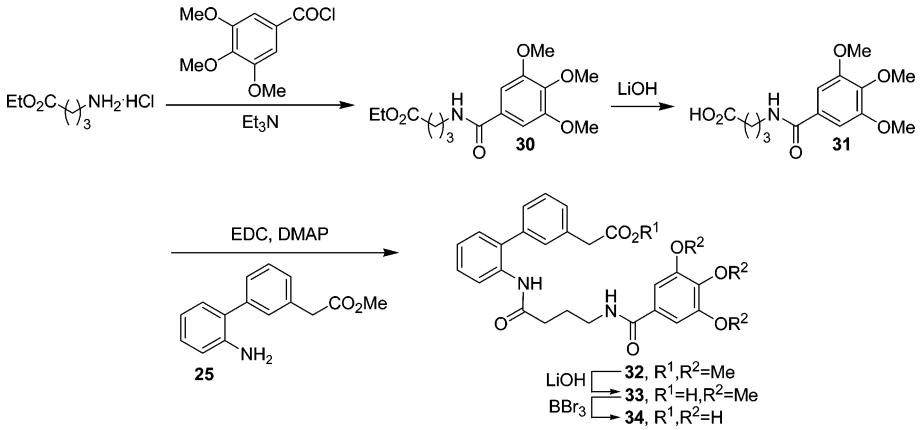

31 with biphenyl **25**, hydrolysis with LiOH, and release of the phenolic hydroxyls with BBr_3 led to carboxylic acid **34**.

We then focused our efforts on a series of compounds containing a carboxylic acid-substituted head part and a pyrogallol type tail part connected by a $-CH_2-$ and $-CH_2CH_2-$ spacer (Scheme 4). The general synthetic route to these novel pyrogallol type compounds is analogous to the one in Scheme 2, whereby 3,4,5-trimethoxyphenyl acetic (**26a**) and propionic acid (**26b**) were employed as starting materials, as well as the appropriately substituted primary amines or anilines. The aminophenyl-thiopheneacetic acid building block **37** was synthesized in two steps starting from 2-thiopheneacetic acid methyl

Scheme 4. Synthetic Routes to 3,4,5-Trimethoxyphenyl Acetic and Propionic Acid Amides **35, 36,** and **38**−**42**[a]

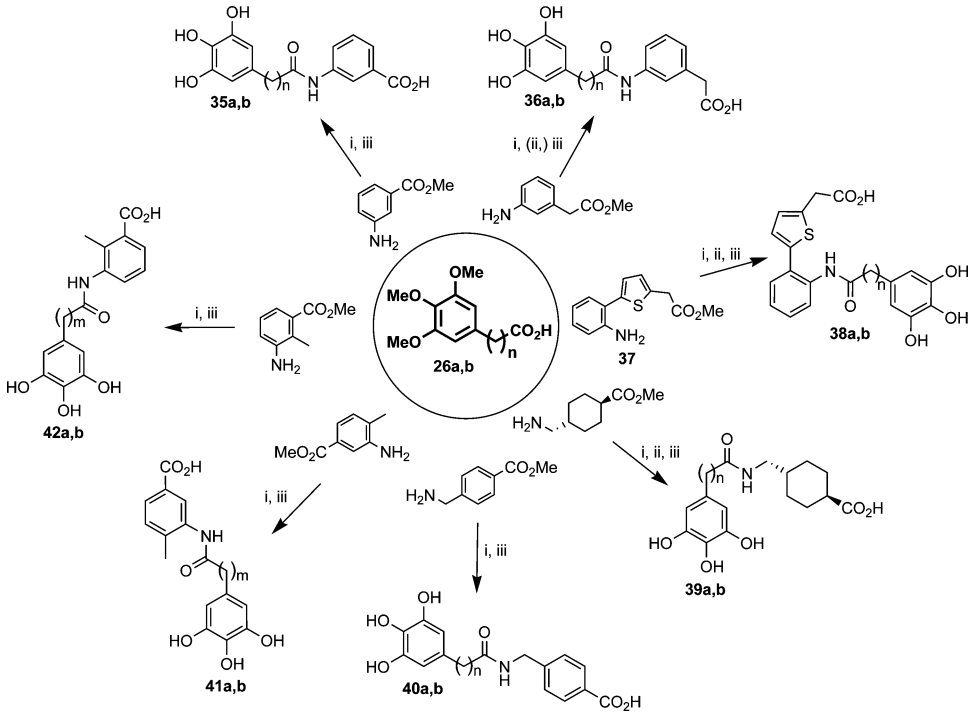

[a] For **a,** $n = 1$ and **b** $n = 2$; (i) EDC, DMAP, Et_3N, CH_2Cl_2; (ii) LiOH, MeOH; (iii) BBr_3, CH_2Cl_2.

Scheme 5. Synthetic Routes to Further **38**-Related Homologous Compounds **44, 46**, **48**, and **50**[a]

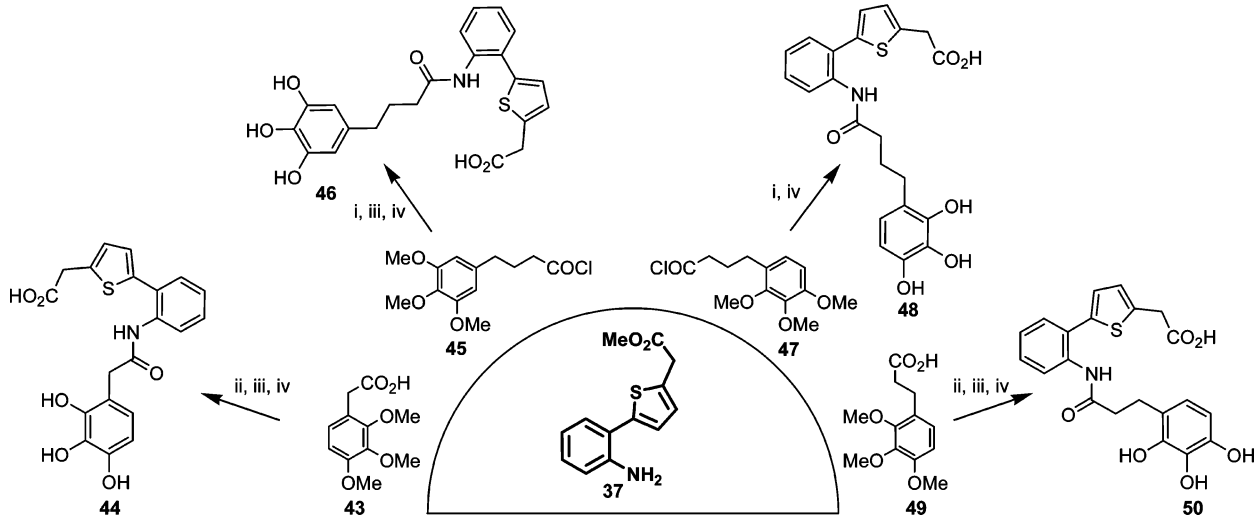

[a] (i) Pyridine, CH_2Cl_2; (ii) EDC, DMAP, Et_3N, CH_2Cl_2; (iii) LiOH, MeOH; (iv) BBr_3, CH_2Cl_2.

ester which was brominated selectively in the 5-position with NBS in glacial acetic acid and $CHCl_3$ followed by a Suzuki type coupling with 2-aminophenylboronic acid in the presence of $Pd(PPh_3)_4$.

Because of the promising assay data on **38b** (Table 1), the phenylthiopheneacetic acid motif was used as the backbone for further homologous and isomeric derivatives outlined in Scheme 5 (**44**, **46**, **48**, and **50**), where spacers and substitution pattern at the pyrogallol subunit (2,3,4- vs 3,4,5-trihydroxy) were initially exchanged. Depending on the nature of the carboxylic acid, either EDC coupling or amidation via the related acid chloride were employed. For carboxylic acid building blocks having any alkyl spacer between the carboxylic acid function and the aromatic ring usually EDC coupling succeeded best. However, in case of **46** and **48** the amidation using the corresponding acid chlorides **45** and **47**, respectively, provided better yields.

Striving toward a more rigid molecular geometry, the number of rotatable bonds was reduced by inserting a double bond or phenyl spacer according to Scheme 6. Again, using **37** as the key building block, the compounds **52**, **54**, **56**, **58**, and **60** were obtained. The synthetic route remained analogous to the one previously described (Scheme 5). Starting materials were either generated from the appropriate trimethoxycinnamic acids (in terms of **51** and **53**) or by Suzuki coupling of the appropriate trimethoxyphenylboronic acids and methyl bromobenzoates followed by subsequent ester hydrolysis with aqueous LiOH solution, and formation of the acid chlorides **55**, **57**, and **59** with oxalyl chloride.

Homologous and isomeric analogues of **56** were then synthesized as in Scheme 7. Synthetic routes to compounds **61**−**65** were adapted from the sequence leading to **56** beginning with the appropriate starting materials. For the generation of the initial trimethoxybiphenyls leading to **63** and **64**, an alternate

Scheme 6. Syntheses of **38**-Related More Rigid Compounds **52, 54**, **56**, **58** and **60**[a]

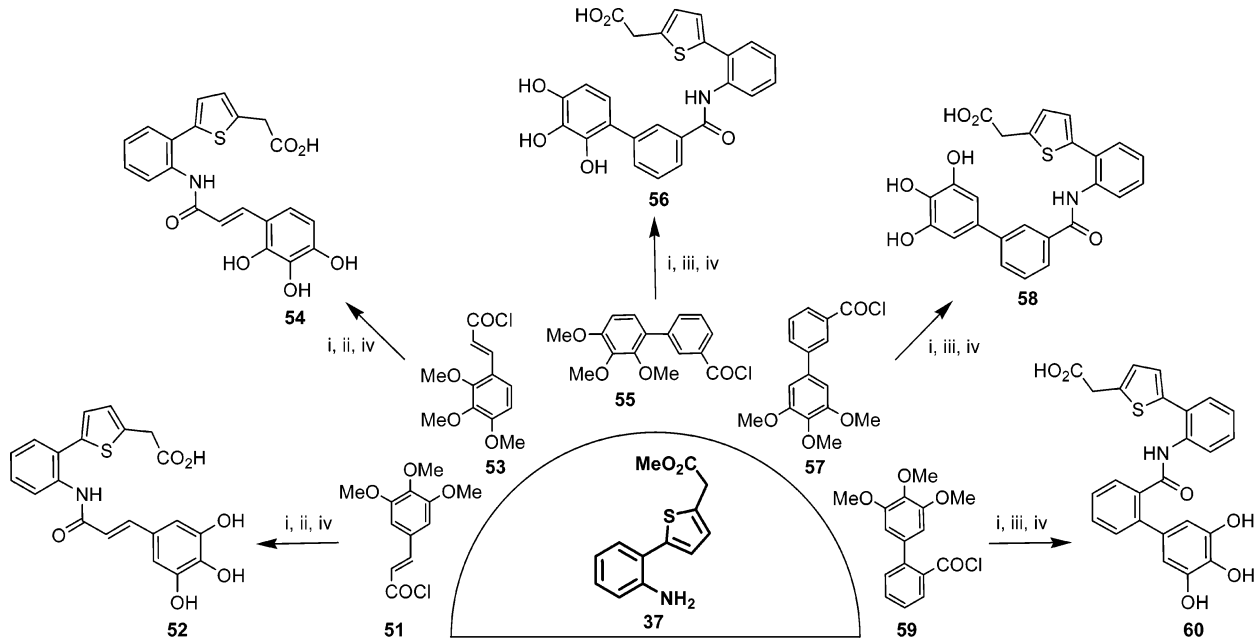

[a] (i) Pyridine, CH_2Cl_2; (ii) LiOH, MeOH; (iii) LiOH, MeCN; (iv) BBr_3, CH_2Cl_2.

Scheme 7. Peripheric Compounds of **56**

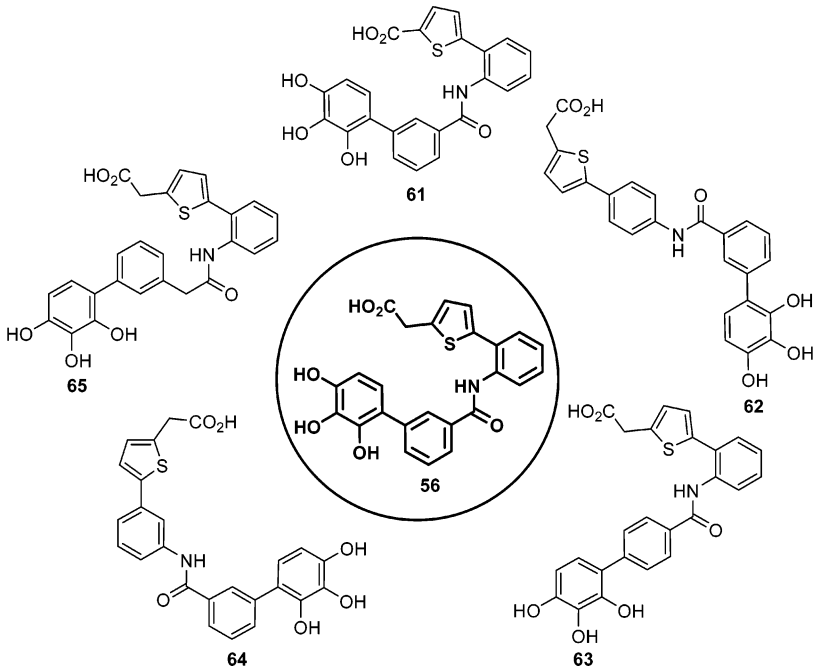

approach using umpoled building blocks (1-bromo-2,3,4-trimethoxybenzene and appropriate borated carboxylic acid esters) had to be applied.

The commonly known substrate-dependency of Suzuki couplings in terms of steric effects and electron density forced us to vary the reaction conditions for the individual coupling steps mentioned above, with respect to solvent, base, or reaction time.

Results and Discussion

The compounds presented here were biologically evaluated employing two *in vitro* assays. A static molecular binding assay was used to determine IC_{50} values or %-inhibition at 100 μM. Here, potential selectin antagonists compete with a polymeric PSGL-1-mimicking ligand (PAA-sLe^X-TYS) for selectin binding. Most candidates were also screened in the dynamic HL-60 cell attachment assay, which measures attachment of HL-60 cells under flow conditions. HL-60 cells provide a complex pattern of selectin ligands on their surface.[32] Discrepancies between results from static molecular binding assay and cell-based assays might be due to hydrodynamic differences and different presentations of selectin ligands in both systems. Overall, compounds with best screening results in both settings are considered to be most promising. Table 1 summarizes the *in vitro* screening data. Since polyphenolic compounds are known for their pH-dependent antioxidative effects,[33] all samples screened in the assays were freshly prepared. As outlined above, a number of catechol and pyrogallol type compounds such as **5** and **4** were screened. Accordingly compound **14**, an analogue of **3** (TBC265), was synthesized (Scheme 1) and tested. The

compound showed IC_{50} values for P-selectin in the nM range and in the lower μM range for L-selectin. However, E-selectin was not inhibited by **14** in the static molecular binding assay. Yet, HL-60 cell attachment for E- and P-selectin was inhibited by **14**. Subsequently, the length of the alkyl spacer between the pyrogallol subunit and the biphenyl moiety was varied. In parallel we switched to an amide connection between the two molecule parts to accelerate and to shorten the chemical access to the target molecules. As compared to **14**, compounds **29a** and **29b** in Scheme 2 have one and two additional methylene groups, respectively, between the amide and pyrogallol motif. In compound **34,** a GABA spacer was introduced between the gallic acid and the biphenyl moiety to further expand the distance (Scheme 3). Out of this set compounds **29a** and **29b** showed the best *in vitro* activity profiles with IC_{50}s for E-, P-, and L-selectin in the lower μM range and comparable inhibition for E- and P-selectin in the cell-based assay. Next, the effect of the biphenyl acetic acid moiety of **29a** and **29b** on selectin binding was investigated. Thus, a library of 14 compounds was synthesized where this moiety was substituted by more simple aromatic carboxylic acids and also by a bioisosteric building block (**26a**,**b**, Scheme 4). Compound **35a** showed a remarkable IC_{50} value for E-selectin in the static molecular binding assay. However, this compound was not active in the dynamic HL-60 cell attachment assay for either E- or P-selectin. Out of this focused library, other compounds displayed low IC_{50} values, whereby compounds **38a**, **40a**, and **40b** gave the best overall *in vitro* activity profile. Due to its overall good activity profile, phenylthiopheneacetic acid analogues **38a** and **38b** were chosen for further optimization. Scheme 5 depicts the synthesis of additional phenylthiopheneacetic acid derivatives. Variation of the spacer length and substitution pattern of pyrogallol (2,3,4- and 3,4,5-trihydroxy) did not result in improved activity, and none of these compounds showed a balanced profile in the static molecular binding and the dynamic HL-60 cell attachment assay. However, compound **48** performed almost as well as **1** (bimosiamose) in the dynamic HL-60 cell attachment assay but was not active in the static molecular binding assay for E-selectin. It was decided to proceed with the general pattern containing the phenylthiopheneacetic acid and pyrogallol subunits and introduce more rigid spacers as the next step (Scheme 6). This strategy led to compounds with a very promising overall profile. The introduction of a double bond gave the regioisomers **52** and **54**. The 2,3,4-trihydroxy-substituted compound **54** demonstrated, as compared to compound **1**, improved inhibition of cell attachment for P-selectin. Inhibition of cell attachment to E-selectin was not significant. Changing the substitution pattern to 3,4,5-trihydroxy, as in compound **52**, resulted in a loss of inhibition for P-selectin attachment but gave moderate inhibition of E-selectin attachment. IC_{50}s for both **52** and **54** were in the lower μM range. The most promising compound of this group was **56**. As compared to **1**, compound **56** showed improved *in vitro* activities in both assays. IC_{50}s were in the lower μM range, and inhibition of HL-60 cell attachment to E- and P-selectin was 61% and 55%, respectively. In **56** the alkyl- or alkene-spacer has been replaced with a 1,3-phenyl group. Substitution pattern of the pyrogallol motif is 2,3,4-trihydroxy. Interestingly, switching the pyrogallol substitution pattern from 2,3,4- (**56**) to 3,4,5-trihydroxy (**58**) diminishes activity. Switching from the 1,3-linked isomer **58** to the 1,2-phenyl-linked compound **60** resulted in poor activity data as well. HL-60 cell attachment to E-selectin was not significant and IC_{50}s particularly for P- and L-selectin were worse than for **58**. This might indicate the capability of the phenyl-spacer to build additional hydrophobic interactions with the selectins. Specific orientation of these groups seems to be crucial for activity. As outlined in Scheme 7, the further influence of small variations of **56** (homologous and isomeric derivatives) was investigated. Hereby the focus was directed to the 2,3,4-trihydroxy substitution of the pyrogallol substructure. From this library, the best activity data were observed for compound **64**. In **64**, the thiophene moiety was connected to the meta position of the amide, rather than the ortho position, as in **56**. The compound showed IC_{50}s in the lower μM range for E- and L-selectin and a nanomolar IC_{50} for P-selectin in the static molecular binding assay. Inhibition of HL-60 cell attachment to E- and P-selectin was 58% and 93%, respectively. Similar activity data were achieved with **61** which is a lower homologue of **56** missing the methylene group between the carboxylic acid and the thiophene moiety. Nanomolar IC_{50}s for P- and L-selectin in the static molecular binding assay were observed for compound **62** wherein the thiophene moiety is connected para to the amide, rather than meta, as in compound **64.** Also for compound **62**, inhibition of HL-60 cell attachment for E- and P-selectin was improved, as compared to molecule **1**. For compound **63**, the 2,3,4-trihydroxyphenyl subunit was connected para to the amide linker. Activities of **63** were also improved as compared to **1**; however, the HL-60 cell attachment data were worse when compared to **56**, **61**, **62**, or **64**. Introduction of a methylene group between the amide group and the pyrogalloylphenyl unit in **56** resulted in the homologous compound **65**. This modification resulted in a loss of activity for E-selectin in both the static molecular binding and the dynamic HL-60 cell attachment assay, whereas IC_{50}s for P- and L-selectin in the static molecular binding assay as well as inhibition of HL-60 cell attachment for P-selectin were noteworthy.

The compounds presented here are the result of a rational hit-finding procedure with focused diversity. While initial hits of a ligand-based approach such as gallic acid derivatives showed moderate biological activity, the homologous compounds such as 3,4,5- or 2,3,4-trihydroxyphenylacetic acid amides showed higher potency. Further modifications led us to compound **56** and related derivatives, e.g., **61**−**64**. These compounds already showed improved *in vitro* activity, as compared to **1**, with IC_{50}s up to the upper nanomolar range and high inhibition values in the dynamic HL-60 cell attachment assay. Having relative molecular weights below 500, these compounds can be considered as small molecules. At this point it seems that hydrophobic interactions might be important for selectin binding. It remains to be analyzed what the functions of the pyrogallol part and of the carboxylic acid are. Compound **64**, for example, seems to be a promising starting point for a more detailed SAR study including comprehensive docking studies in the course of hit-to-lead and lead optimization programs and is the subject of ongoing research activities. However, it should be mentioned that obtaining a meaningful SAR for compounds which bind to selectins is a particular challenge. Beside other proposed binding regions, the surface of the C-type lectin domain of selectins has been identified as important binding site for natural, sLe^X-bearing ligands. Indeed, the selectin antagonists presented herein are supposed to address this binding site, which is also reflected by the type of molecular binding assay described here. In contrast to the shape of binding sites of many other drug targets, selectins provide a shallow surface with highly flexible amino acids to their interaction partners, rather than a buried cavity with rotationally more restricted amino acids. This, of course, impacts drug discovery of synthetic small molecule selectin antagonists. Since even

structurally similar ligands show an increased probability to bind to selectins with different binding modes, clear structure−activity-relationship may be difficult to obtain.

The novel class of synthetic selectin antagonists presented herein are polyphenolic compounds tethered to carboxylic acid through a variety of structural units. Phenolic and polyphenolic compounds are common in many natural products, food constituents, and marketed drugs. Members of this compound class can be found in green tea, red wine, grapes, apples, and chocolate, for instance, and they are believed to be responsible for protective antioxidative, anticancer, antiinflammatory, and cardiovascular protecting effects, commonly known as the French paradox.[8,34] Consequently, pharmacological action of natural polyphenolics is the subject of intensive research. The inhibitory activity of short peptides against P-selectin, found by phage display, could be improved to nanomolar IC_{50} values by the N-terminal attachment of gallic acid.[35] Accordingly, the authors investigated the inhibitory effect of **5** on P-selectin.[8] It could be shown, that molecule **5** binds to P-selectin in a relative potent manner. However, the authors did not observe binding to E-selectin and binding to L-selectin was moderate.

In conclusion, novel, rationally designed synthetic small molecules with nanomolar *in vitro* activity against E-, P-, and L-selectin and with a relative molecular weight below 500 have been presented. Current research activities are directed toward further medicinal chemistry including comprehensive computational investigations in order to optimize pharmacodynamic and pharmacokinetic properties of this novel class of compounds, and results from these studies will be disclosed in due course.

Experimental Section

Computational Chemistry. Molecular simulations such as stochastic conformational searches, setup of 3D databases of vendor compound collections, pharmacophore searches, and molecular alignment have been performed with MOE of the Chemical Computing Group Inc.[20] The MMFF94x force field has been applied in all energy-based calculation. The flexible alignment procedure was applied with equally weighted similarity terms for hydrogen-bond donors and acceptors, aromaticity, acid/base, and volume.

Chemistry. Solvents and reagents were used as received from commercial distributors without further purification. Anhydrous reactions were conducted under a nitrogen atmosphere. Proton NMR spectra were recorded at a 400 MHz Bruker Avance 400. Chemical shifts δ are reported in ppm units. Molecular mass was determined by liquid chromatography mass spectrometry (LC/MS) using an LCQ Advantage ion trap mass spectrometer from Thermo Finnigan equipped with an electrospray interface and connected to a Surveyor HPLC (Thermo Finnigan). Positive and negative ion mass spectra were recorded (mass range m/z 150−1000) in normal scan mode. Preparative reversed phase (RP) HPLC was run on a Shimadzu LC8A instrument using a Phenomenex Synergi 10 μ Hydro RP 80A (15 mm i.d. × 250 mm) C-18 column. The flow rate was 5 mL/min, the mobile phase A was water and the mobile phase B acetonitrile, containing 0.05% TFA each as modifier. Purity was determined using a Shimadzu 10ADvp instrument with C18 RP column. Two methods were applied: method A using a gradient of water and acetonitrile (from 5% B to 95% B in 8.5 min) and method B using a gradient of water and methanol (from 5% B to 95% B in 4.5 min followed by 5 min at 95% B). Each solvent contained 0.05% TFA, flow rate was 1.5 mL/min and UV detection was performed at 254 nm. Pure fractions were pooled and lyophilized. For purifications with preparative radial thin layer chromatography a Harrison Research Chromatotron No. 7924 T was employed using glass disks coated with silica gel $60PF_{254}$ (containing gypsum from Merck, Germany; 1 mm, 2 mm, or 4 mm layer thickness) as stationary phase. The tetrasaccharide sLe^X has been acquired from Carbohydrate Synthesis Ltd.

{2′-[(3,4,5-Trihydroxybenzoyl)oxy]-1,1′-biphenyl-3-yl}-acetic Acid (14). Step 1. (3-Bromo-phenyl)-acetic acid (**16**, 2.15 g, 10 mmol) was dissolved in anhydrous DMF (12.5 mL) at rt, and sodium bicarbonate (2.1 g, 25 mmol) was added, followed by slow addition of benzyl bromide (2.99 mL, 25 mmol). The reaction was stirred at 100 °C overnight and then mixed with water and extracted with EtOAc (three times). The combined extracts were washed with brine, dried with Na_2SO_4, and concentrated. The crude product was purified by preparative radial chromatography (CyH/EtOAc 3:1) to obtain benzyl (3-bromophenyl)-acetate (**17**, 3.05 g, quant.) as a colorless oil. ^{1}H NMR (400 MHz, $CDCl_3$): 3.62 (s, 2 H); 5.12 (s, 2 H); 7.14−7.22 (m, 2 H); 7.26−7.41 (m, 6 H) 7.43 (s, 1 H).

Step 2. Phenol (941 mg, 10.0 mmol) was dissolved in dichloromethane (80 mL), PPTS (251 mg, 1.0 mmol) and then 3,4-dihydro-2*H*-pyran (2.75 mL, 30.0 mmol) were added, and the mixture was stirred at rt under nitrogen overnight. The reaction was mixed with water and extracted with EtOAc (three times). The combined extracts were washed with half-saturated brine, dried with Na_2SO_4, and then concentrated. The crude 2-phenoxytetrahydro-2*H*-pyran (1.78 g, quant.) was obtained as a white solid. ^{1}H NMR (400 MHz, $CDCl_3$): 1.51−1.73 (m, 3 H); 1.81−1.88 (m, 2 H); 1.94−2.06 (m, 1 H); 3.55−3.62 (m, 1 H); 3.90 (Ψtd, 1 H, J_1 = 9.0 Hz, J_2 = 3.0 Hz); 5.40 (Ψt, 1 H, J = 3.0 Hz); 6.96 (t, 1 H, J = 7.3 Hz); 7.03 (d, 2 H, J = 8.0 Hz); 7.26 (t, 2 H, J = 7.6 Hz).

2-Phenoxytetrahydro-2*H*-pyran (1.00 g, 5.6 mmol) was dissolved in anhydrous THF (20 mL) under a N_2 atmosphere, and then the solution was cooled to −78 °C. A solution of *n*-BuLi in hexane (5.25 mL of a 1.6 M solution, 8.40 mmol) was added slowly, and the reaction mixture was stirred for 15 min at −78 °C and then an additional 30 min at rt. The mixture was cooled again to −78 °C before triisopropyl borate (3.25 mL, 14 mmol) was added. The reaction mixture was slowly warmed up to rt and stirred for additional 2 h. The reaction was mixed with water and then extracted with EtOAc (three times). The combined extracts were washed with brine, dried with Na_2SO_4, and concentrated to obtain 2-(tetrahydro-2*H*-pyran-2-yloxy)phenyl]boronic acid (**18**, 1.35 g, 79%) as an adhesive off-white solid, which was used without further purification.

Step 3. [2-(Tetrahydro-2*H*-pyran-2-yloxy)phenyl]boronic acid (**18**, 153 mg, 0.69 mmol) was dissolved in toluene (10.0 mL) and ethanol (1.5 mL), and the mixture was treated with tetrakis-(triphenylphosphine)-palladium(0) (50 mg, 0.04 mmol) and aq Na_2CO_3 (2.0 mL of a 2.5 M solution, 5.0 mmol) followed by addition of benzyl (3-bromophenyl)-acetate (**17**, 200 mg, 0.65 mmol) in toluene (10.0 mL). The reaction mixture was degassed under nitrogen (five times), flooded with N_2 again and stirred vigorously for 2 h at 100 °C. The resulting mixture was then filtered through silica gel, which was washed with EtOAc. The combined filtrates were concentrated, and the crude product was purified by preparative radial chromatography (CyH/EtOAc 1:1) to obtain an inseparable mixture of benzyl [2′-(tetrahydro-2*H*-pyran-2-yloxy)-1,1′-biphenyl-3-yl]-acetate (**19**) and starting material **17** (403 mg, about 1:1) as a colorless oil.

Step 4. Benzyl [2′-(tetrahydro-2*H*-pyran-2-yloxy)-1,1′-biphenyl-3-yl]-acetate (**19**, 156 mg, 0.7 mmol) was dissolved in MeOH (20 mL) at rt. *p*TsOH·H_2O (4.0 mg, 0.02 mmol) was added, and the reaction mixture was stirred for 2 h at 40 °C. A mixture of EtOAc (10 mL) and brine (10 mL) was added to the cooled reaction and mixed well. The aqueous phase was extracted with EtOAc, and the combined organic phases were washed with brine, dried with Na_2SO_4, and concentrated under reduced pressure. The crude product was purified by preparative radial chromatography (CyH/EtOAc 3:1) to obtain benzyl (2′-hydroxy-1,1′-biphenyl-3-yl)-acetate (**20**, 88 mg, 76%) as a colorless oil. ^{1}H NMR (400 MHz, $CDCl_3$): 3.72 (s, 2 H); 5.14 (s, 2 H); 5.15 (br. s, 1 H); 6.92−7.00 (m, 2 H); 7.16−7.23 (m, 2 H) 7.28−7.47 (m, 9 H).

Step 5. Benzyl (2′-hydroxy-1,1′-biphenyl-3-yl)-acetate (**20**, 46 mg, 0.14 mmol) was dissolved in anhydrous dichloromethane (1.0 mL) and Et_3N (29 μL, 0.21 mmol) was added. The solution was stirred for 5 min at rt, and then 5-(chlorocarbonyl) benzene-1,2,3-triyl triacetate (**21**, 50 mg, 0.16 mmol) was added. The reaction

mixture was stirred another 30 min at rt, then quenched with sat. aqueous NH_4Cl solution and extracted with dichloromethane. The extracts were combined and washed with brine, dried with Na_2SO_4, and then concentrated under reduced pressure. The crude product was purified by preparative radial chromatography (CyH/EtOAc 3:1) to obtain 3′-[2-(benzyloxy)-2-oxoethyl]-1,1′-biphenyl-2-yl 3,4,5-tris(acetyloxy) benzoate (**22**, 55 mg, 64% yield) as an adhesive colorless solid. ^{1}H NMR (400 MHz, $CDCl_3$): 2.24 (s, 6 H); 2.27 (s, 3 H); 3.61 (s, 2 H); 5.06 (s, 2 H); 7.16−7.41 (m, 13 H); 7.74 (s, 2 H).

Step 6. 3′-[2-(Benzyloxy)-2-oxoethyl]-1,1′-biphenyl-2-yl 3,4,5-tris(acetyloxy) benzoate (**22**, 55 mg, 0.09 mmol) was dissolved in acetone (0.5 mL) and then treated with an aqueous NH_3 solution (58 μL, 1.0 mmol). The reaction mixture was stirred for 15 min at rt and then quenched with a 1 N aq HCl solution (pH ∼ 3). The aq phase was extracted with EtOAc, and the combined organic phases were dried with Na_2SO_4 and then concentrated under reduced pressure. The crude 3′-[2-(benzyloxy)-2-oxoethyl]-1,1′-biphenyl-2-yl 3,4,5-trihydroxybenzoate (**23**) was dissolved in EtOAc (1.0 mL), and Pd/C (10 mg) was added. The resulting mixture was carefully evacuated, flooded with hydrogen three times, and then stirred under a hydrogen atmosphere at rt overnight. The reaction system was evacuated again and flushed with N_2. The reaction mixture was filtered and then concentrated under reduced pressure. The crude product was purified by preparative RP HPLC to obtain {2′-[(3,4,5-trihydroxybenzoyl)oxy]-1,1′-biphenyl-3-yl} acetic acid (**14**, 9 mg, 14%). ^{1}H NMR (400 MHz, CD_3CN): 3.59 (s, 2 H); 7.05 (s, 2 H); 7.21 (d, 1 H, J = 7.6 Hz); 7.27 (d, 1 H, J = 7.8 Hz); 7.32 (t, 1 H, J = 7.6 Hz); 7.34−7.49 (m, 5 H).

{2′-[3-(3,4,5-Trihydroxy-phenyl)-propionylamino]-biphenyl-3-yl}-acetic Acid (29b). Step 1. Tetrakis-(triphenylphosphine)-palladium(0) (30 mg, 0.025 mmol) and Na_2CO_3 decahydrate (944 mg, 3.30 mmol dissolved in 1.2 mL of H_2O) were added to ethanol (0.8 mL), followed by a solution of 2-amino-benzeneboronic acid (201 mg, 1.30 mmol) in toluene (6.0 mL). The reaction mixture was carefully degassed under nitrogen five times, and then flooded with N_2 again. A solution of (3-bromo-phenyl)-acetic acid methyl ester (**24**, 270 mg, 1.18 mmol) in toluene (6.0 mL) was then added, and the reaction mixture was degassed again (five times) and then stirred overnight at 100 °C. The reaction mixture was then partitioned between EtOAc and brine (1:1), and then the aqueous phase was extracted with EtOAc (three times). The combined organic phases were washed with brine, dried with Na_2SO_4, and concentrated. The crude product was purified by preparative radial chromatography (CyH/EtOAc 3:1) to obtain (2′-amino-biphenyl-3-yl)-acetic acid methyl ester (**25**, 304 mg, 81%) as an orange oil. ^{1}H NMR (400 MHz, $CDCl_3$): 3.66 (s, 2 H); 3.69 (s, 3 H); 3.62−3.86 (br. s, 2 H); 6.75 (d, 1 H, J = 8.1 Hz); 6.80 (t, 1 H, J = 7.3 Hz); 7.11 (d, 1 H, J = 7.3 Hz); 7.15 (d, 1 H, J = 8.1 Hz); 7.22−7.26 (br. m, 1 H); 7.32−7.42 (m, 3 H).

Step 2. EDC hydrochloride (61 mg, 0.32 mmol) and Et_3N (44 μL, 0.32 mmol) were mixed with anhydrous dichloromethane (1.0 mL), and the resulting mixture was stirred under nitrogen for 5 min at rt. 3-(3,4,5-Trimethoxy-phenyl)-propionic acid (**26b**, 55 mg, 0.23 mmol) and DMAP (2 mg, 0.02 mmol) were added, and the resulting solution was stirred for 15 min. (2′-Amino-biphenyl-3-yl)-acetic acid methyl ester (**25**, 50 mg, 0.21 mmol) was then added, and the reaction mixture was stirred overnight at rt and then quenched with water. The aq phase was extracted with dichloromethane (three times), and the combined organic phases were washed with brine, dried with Na_2SO_4, and concentrated. The crude product was purified by preparative radial chromatography (EtOAc/CyH 1:1) to obtain {2′-[3-(3,4,5-trimethoxy-phenyl)-propionylamino]-biphenyl-3-yl}-acetic acid methyl ester (**27b**, 46 mg, 48%) as a yellow oil. ^{1}H NMR (400 MHz, $CDCl_3$): 2.50 (t, 2 H, J = 7.6 Hz); 2.90 (t, 2 H, J = 7.7 Hz); 3.64 (s, 2 H); 3.65 (s, 3 H); 3.77 (s, 6 H); 3.78 (s, 3 H); 6.38 (s, 2 H); 7.09−7.18 (m, 3 H); 7.19−7.28 (m, 3 H); 7.34 (d, 1 H, J = 8.1 Hz); 7.38 (d, 1 H, J = 7.8 Hz); 8.31 (br. d, 1 H, J = 7.8 Hz).

Step 3. {2′-[3-(3,4,5-Trimethoxy-phenyl)-propionylamino]-biphenyl-3-yl}-acetic acid methyl ester (**27b**, 35 mg, 0.075 mmol) was dissolved in MeOH (2.5 mL) at rt, and aq LiOH (385 μL of a 1 M solution, 385 μmol) was added. The reaction mixture was stirred for 17 h at rt and then quenched with 1 M aq HCl (pH ∼ 3), with cooling as necessary. The mixture was then extracted with EtOAc (three times), and the extracts were combined, washed with water and then brine, dried with Na_2SO_4, and then concentrated, to obtain {2′-[3-(3,4,5-trimethoxy-phenyl)-propionylamino]-biphenyl-3-yl}-acetic acid (**28**, 36 mg, quant.) as an adhesive white solid that was used without further purification. ^{1}H NMR (400 MHz, $CDCl_3$): 2.46 (t, 2 H, J = 7.2 Hz); 2.86 (t, 2 H, J = 7.3 Hz); 3.65 (s, 2 H); 3.74 (s, 6 H); 3.77 (s, 3 H); 6.36 (s, 2 H); 7.09−7.22 (m, 5 H); 7.25 (d, 1 H, J = 7.6 Hz); 7.30−7.40 (m, 2 H); 8.28 (br. d, 1 H, J = 8.1 Hz).

Step 4. {2′-[3-(3,4,5-Trimethoxy-phenyl)-propionylamino]-biphenyl-3-yl}-acetic acid (**28**, 33 mg, 0.073 mmol) was dissolved in anhydrous dichloromethane (2.5 mL) under nitrogen, and then the solution was cooled to −78 °C. A solution of BBr_3 in dichloromethane (440 μL of a 1 M solution, 0.44 mmol) was added dropwise. The reaction mixture was stirred for 30 min at −78 °C, warmed slowly to rt, and stirred an additional 90 min at rt. The reaction was quenched by dropwise addition of ice−water, the layers were separated, and the aq phase was extracted with EtOAc (three times). The combined organic phases were washed with water and then brine, dried with Na_2SO_4, and then concentrated. The crude product was purified by preparative RP HPLC to obtain {2′-[3-(3,4,5-trihydroxy-phenyl)-propionylamino]-biphenyl-3-yl}-acetic acid (**29b**, 21 mg, 71%). ^{1}H NMR (400 MHz, CD_3OD): 2.48 (t, 2 H, J = 7.6 Hz); 2.71 (t, 2 H, J = 7.6 Hz); 3.69 (s, 2 H); 6.24 (s, 2 H); 7.17 (dt, 1 H, J_1 = 7.6 Hz, J_2 = 1.3 Hz); 7.28−7.42 (m, 6 H); 7.60 (d, 1 H, J = 7.6 Hz). MS (ESI) m/z 408.1 ($[M + H]^+$).

{2′-[4-(3,4,5-Trihydroxy-benzoylamino)-butyrylamino]-biphenyl-3-yl}-acetic Acid (34). Step 1. 4-Amino-butyric acid ethyl ester hydrochloride (3.98 g, 23.74 mmol) was dissolved in anhydrous dichloromethane (120 mL) at rt under nitrogen, and triethylamine (8.30 mL, 59.55 mmol) was added. The reaction mixture was stirred for 15 min at rt, 3,4,5-trimethoxy-benzoyl chloride (6.58 g, 28.53 mmol) was added in portions, and the mixture was stirred for additional 24 h at rt. The reaction mixture was quenched with methanol, filtered through a short pad of silica gel with EtOAc/CyH (3:1), and concentrated. The crude product was purified by flash chromatography (EtOAc/CyH 2:1 and then 3:1) to obtain 4-(3,4,5-trimethoxy-benzoylamino)-butyric acid ethyl ester (**30**, 4.48 g, 58%) as a white solid. ^{1}H NMR (400 MHz, $CDCl_3$): 1.22 (t, 3 H, J = 7.1 Hz); 1.95 (Ψquint, 2 H, J = 6.5 Hz); 2.44 (t, 2 H, J = 6.5 Hz); 3.48 (td, 2 H, J_1 = 6.5 Hz, J_2 = 5.8 Hz); 3.85 (s, 3 H); 3.89 (s, 6 H); 4.10 (q, 2 H, J = 7.1 Hz); 6.72 (br. s, 1 H); 7.02 (s, 2 H).

Step 2. 4-(3,4,5-Trimethoxy-benzoylamino)-butyric acid ethyl ester (**30**, 4.48 g, 13.79 mmol) was dissolved in acetonitrile (100 mL) at rt, and a solution of aq LiOH (41.4 mL of a 1 M solution, 41.4 mmol) was added. The reaction mixture was stirred for 18 h at rt and then quenched by addition of 1 M aq HCl (50 mL), with cooling as necessary. The mixture was then extracted with chloroform (three times), and the combined organic phases were washed with brine, dried with Na_2SO_4, and concentrated, to obtain 4-(3,4,5-trimethoxy-benzoylamino)-butyric acid (**31**, 4.07 g, 99%) as a white solid. ^{1}H NMR (400 MHz, $CDCl_3$): 1.94 (Ψquint, 2 H, J = 6.7 Hz); 2.46 (t, 2 H, J = 6.7 Hz); 3.50 (br. td, 2 H); 3.85 (s, 3 H); 3.88 (s, 6 H); 6.61 (br. s, 1 H); 7.00 (s, 2 H).

Step 3. EDC hydrochloride (55 mg, 0.29 mmol) and Et_3N (40 μL, 0.29 mmol) were mixed with anhydrous dichloromethane (1.0 mL) under nitrogen, and the resulting solution was stirred for 5 min at rt. 4-(3,4,5-Trimethoxy-benzoylamino)-butyric acid (**31**, 63 mg, 0.21 mmol) was added and then DMAP (2 mg, 0.02 mmol), and the resulting solution was stirred for 10 min. (2′-Amino-biphenyl-3-yl)-acetic acid methyl ester (**25**, 46 mg, 0.19 mmol) was added, and the reaction was stirred for 15 h at rt. The reaction was then quenched by addition of sat. aq NH_4Cl and water. The layers were separated, and the aq phase was extracted with dichloromethane (three times). The combined organic phases were washed with water and then brine, dried with Na_2SO_4, and concentrated.

The crude product was purified by preparative radial chromatography (EtOAc/CyH 3:1 and then 6:1) to obtain {2′-[4-(3,4,5-trimethoxy-benzoylamino)-butyrylamino]-biphenyl-3-yl}-acetic acid methyl ester (**32**, 36 mg, 37%) as a yellowish oil. ^{1}H NMR (400 MHz, $CDCl_3$): 1.91−2.00 (m, 2 H); 2.43 (t, 2 H, J = 6.2 Hz); 3.41−3.50 (m, 2 H); 3.64 (s, 2 H); 3.68 (s, 3 H); 3.81 (s, 6 H); 3.83 (s, 3 H); 7.06 (s, 2 H); 7.13−7.27 (m, 5 H); 7.29 (t, 1 H, J = 7.7 Hz); 7.35−7.45 (m, 3 H); 8.11 (d, 1 H, J = 8.1 Hz).

Step 4. {2′-[4-(3,4,5-Trimethoxy-benzoylamino)-butyrylamino]-biphenyl-3-yl}-acetic acid methyl ester (**32**, 36 mg, 0.07 mmol) was dissolved in MeOH (2.0 mL) at rt, and a solution of aq LiOH (490 μL of a 1 M solution, 0.49 mmol) was added. The reaction mixture was stirred for 17 h at rt, and then the reaction mixture was partitioned between chloroform and 1 M hydrochloric acid. The aq phase was separated and extracted with chloroform (three times). The combined organic phases were washed with brine, dried with Na_2SO_4, and concentrated, to obtain {2′-[4-(3,4,5-trimethoxy-benzoylamino)-butyryl-amino]-biphenyl-3-yl}-acetic acid (**33**, 37 mg of crude product, quant.) as a brown solid. ^{1}H NMR (400 MHz, $CDCl_3$): 1.97 (Ψquint, 2 H, J = 6.9 Hz); 2.38 (t, 2 H, J = 7.3 Hz); 3.51−3.60 (m, 2 H); 3.65 (s, 2 H); 3.83 (s, 6 H); 3.84 (s, 3 H); 6.67 (br. s, 1 H); 6.99 (s, 2 H); 7.15 (t, 1 H, J = 7.3 Hz); 7.20−7.30 (m, 4 H); 7.32 (t, 1 H, J = 7.8 Hz); 7.37 (s, 1 H), 7.44 (t, 1 H, J = 7.4 Hz); 8.27 (d, 1 H, J = 8.3 Hz).

Step 5. {2′-[4-(3,4,5-Trimethoxy-benzoylamino)-butyryl-amino]-biphenyl-3-yl}-acetic acid (**33**, 37 mg, 0.07 mmol) was dissolved in anhydrous dichloromethane (1.0 mL) under nitrogen, the solution was cooled to −78 °C, and then BBr_3 (62 μL, 0.66 mmol) was added dropwise. The reaction mixture was stirred for 30 min at −78 °C, warmed slowly to rt, and stirred an additional 2 h at rt. The reaction mixture was then cooled to 0 °C and quenched by dropwise addition of water. The resulting mixture was partitioned between water and EtOAc. The aq phase was extracted with EtOAc (two times) and dichloromethane (two times), and the combined organic phases were washed with brine, dried with Na_2SO_4, and concentrated, to obtain {2′-[4-(3,4,5-trihydroxy-benzoylamino)-butyrylamino]-biphenyl-3-yl}-acetic acid (**34**, 17 mg, 53%) as a white solid. ^{1}H NMR (400 MHz, CD_3CN): 1.72−1.82 (m, 2 H); 2.23 (t, 2 H, J = 7.4 Hz); 3.27−3.35 (m, 2 H); 3.63 (s, 2 H); 6.60 (s, 1 H); 6.84 (s, 2 H); 7.11 (br. s, 1 H); 7.18−7.37 (m, 5 H); 7.41 (t, 1 H, J = 7.6 Hz); 7.79 (s, 1 H); 7.86 (d, 1 H, J = 8.3 Hz). MS (ESI) m/z 465.4 ($[M + H]^+$).

(5-{2-[(2′,3′,4′-Trihydroxy-biphenyl-3-carbonyl)-amino]-phenyl}-thiophen-2-yl)-acetic Acid (56). Step 1. Thiophene-2-yl-acetic acid methyl ester (2.0 g, 12.8 mmol) was dissolved in anhydrous chloroform (9.0 mL) and glacial acetic acid (9.0 mL) under nitrogen, and *N*-bromosuccinimide (2.3 g, 13.0 mmol) was added in portions. The mixture was stirred for 3 d at rt, and then water was added to the reaction mixture. The layers were separated, and the aq phase was extracted with dichloromethane. The combined organic phases were extracted several times with a 1 M aq NaOH and then water followed by brine, dried with Na_2SO_4, and concentrated. The crude product was purified by preparative radial chromatography (CyH/EtOAc 5:1] to obtain (5-bromo-thiophen-2-yl)-acetic acid methyl ester as a yellow oil (2.46 g, 81%) which was used without any further purification. ^{1}H NMR (400 MHz, $CDCl_3$): 3.71 (s, 3 H); 3.75 (s, 2 H); 6.67 (d, 1 H, J = 3.8 Hz); 6.88 (d, 1 H, J = 3.8 Hz).

Step 2. Tetrakis-(triphenylphosphine)-palladium(0) (289 mg, 0.25 mmol) and Na_2CO_3 decahydrate (4.0 g, 14.0 mmol) were dissolved in water (5.2 mL) and ethanol (3.7 mL) under nitrogen, and the mixture was treated with a solution of 2-amino-benzeneboronic acid hydrochloride (910 mg, 5.25 mmol) in toluene (52 mL). The reaction mixture was carefully degassed under nitrogen five times and flooded with N_2 again. A solution of (5-bromo-thiophen-2-yl)-acetic acid methyl ester (1.17 g, 5.0 mmol) in toluene (4.5 mL) was added, and the reaction was degassed again (five times) and stirred for 22 h at 100 °C. The reaction mixture was then partitioned between EtOAc and brine, and the layers were separated. The aq phase was extracted with EtOAc (three times), and the combined organic phases were washed with water and then brine, dried with Na_2SO_4, and concentrated. The crude product was purified by preparative radial chromatography (CyH/EtOAc 5:1] to obtain [5-(2-amino-phenyl)-thiophen-2-yl]-acetic acid methyl ester (**37**, 634 mg, 51%) as a brown oil. ^{1}H NMR (400 MHz, $CDCl_3$): 3.73 (s, 3 H); 3.83 (s, 2 H); 3.92−4.07 (br. s, 2 H); 6.74 (d, 1 H); 6.76 (td, 1 H, J_1 = 7.6 Hz, J_2 = 1.3 Hz); 6.92 (d, 1 H, J = 3.5 Hz); 7.02 (d, 1 H, J = 3.5 Hz); 7.11 (td, 1 H, J_1 = 7.6 Hz, J_2 = 1.5 Hz); 7.23 (dd, 1 H, J_1 = 7.6 Hz, J_2 = 1.5 Hz). MS (ESI) m/z 248.1 ($[M + H]^+$). HPLC t_R = 8.36 min, 84% pure.

Step 3. A solution of 2,3,4-trimethoxyphenylboronic acid (1.40 g, 6.60 mmol) in toluene (15 mL) under nitrogen was treated with EtOH (2.0 mL), tetrakis-(triphenylphosphine)-palladium(0) (208 mg, 0.18 mmol), and then Na_2CO_3 decahydrate (4.81 g, 16.80 mmol) in water (5.2 mL). The resulting mixture was carefully degassed under nitrogen (five times), a solution of methyl-3-bromobenzoate (1.29 g, 6.00 mmol) in toluene (9.0 mL) was added by syringe, and the resulting mixture was again carefully degassed and stirred overnight at 100 °C under nitrogen. The mixture was partitioned between brine/EtOAc (1:1), and the layers were separated. The aq phase was extracted with EtOAc (three times), and the combined organic phases were washed with brine, dried with Na_2SO_4, and concentrated. The crude product was purified by preparative radial chromatography (EtOAc/CyH 1:5) to obtain 2′,3′,4′-trimethoxy-biphenyl-3-carboxylic acid methyl ester (1.07 g, 58%) as an yellowish oil. ^{1}H NMR (400 MHz, $CDCl_3$): 3.66 (s, 3 H); 3.89 (s, 3 H); 3.92 (s, 6 H); 6.74 (d, 1 H, J = 8.6 Hz); 7.03 (d, 1 H, J = 8.6 Hz); 7.44 (t, 1 H, J = 7.8 Hz); 7.70 (d, 1 H, J = 7.6 Hz); 7.97 (d, 1 H, J = 7.8 Hz); 8.15 (br. s, 1 H).

Step 4. 2′,3′,4′-Trimethoxy-biphenyl-3-carboxylic acid methyl ester (566 mg, 1.87 mmol) was dissolved in acetonitrile (19 mL) at rt, and aq LiOH (9.36 mL of a 1 M solution, 9.36 mmol) was added. The reaction mixture was stirred overnight at rt and then quenched by addition of 1 M aq HCl (pH ∼ 3), with cooling as necessary. The mixture was extracted with EtOAc (three times), and the combined extracts were washed with brine, dried with Na_2SO_4, and concentrated. The crude product was crystallized from EtOAc/CyH 1:3 to obtain 2′,3′,4′-trimethoxy-biphenyl-3-carboxylic acid (392 mg, 72%) as a white solid. ^{1}H NMR (400 MHz, CD_3OD): 3.68 (s, 3 H); 3.93 (br. s, 6 H); 6.92 (d, 1 H, J = 8.6 Hz); 7.11 (d, 1 H, J = 8.6 Hz); 7.54 (t, 1 H, J = 7.7 Hz); 7.75 (d, 1 H, J = 7.6 Hz); 8.01 (d, 1 H, J = 7.8 Hz); 8.18 (br. s, 1 H).

Step 5. 2′,3′,4′-Trimethoxy-biphenyl-3-carboxylic acid (107 mg, 0.37 mmol) was dissolved in anhydrous dichloromethane (3.0 mL) under nitrogen, and anhydrous DMF (3 drops, cat. amount) was added. Oxalyl chloride (42 μL, 0.48 mmol) was then added slowly, keeping the temperature at ca. 15 °C (water bath), and the turbid mixture was stirred for additional 2 h at rt. The resulting solution of crude 2′,3′,4′-trimethoxy-biphenyl-3-carbonyl chloride (**55**) was added to an ice-cooled solution of [5-(2-amino-phenyl)-thiophen-2-yl]-acetic acid methyl ester (**37**, 70 mg, 0.28 mmol) in anhydrous dichloromethane (4.5 mL) and anhydrous pyridine (0.75 mL). The cooling bath was removed, and the reaction was stirred for 3 h at rt and then mixed with an ice-cooled solution of 1 M aq HCl. The mixture was then extracted with dichloromethane (three times), and the combined organic phases were washed with brine, dried with Na_2SO_4, and concentrated. The crude product was purified by preparative radial chromatography (EtOAc/CyH 1:3, later 1:2) to obtain (5-{2-[(2′,3′,4′-trimethoxy-biphenyl-3-carbonyl)-amino]-phenyl}-thiophen-2-yl)-acetic acid methyl ester (96 mg, 65%) as an adhesive brownish solid. ^{1}H NMR (400 MHz, $CDCl_3$): 3.64 (s, 3 H); 3.71 (s, 3 H); 3.84 (s, 2 H); 3.90 (s, 3 H); 3.92 (s, 3 H); 6.75 (d, 1 H, J = 8.8 Hz); 6.97 (d, 1 H, J = 3.5 Hz); 7.01 (d, 1 H, J = 8.8 Hz); 7.03 (d, 1 H, J = 3.5 Hz); 7.16 (br. t, 1 H, J = 7.6 Hz); 7.36−7.43 (m, 2 H); 7.46 (t, 1 H, J = 7.7 Hz); 7.67 (Ψdd, 2 H, J_1 = 7.6 Hz, J_2 = 1.5 Hz); 7.91 (br. s, 1 H); 8.41 (br. s, 1 H); 8.50 (d, 1 H, J = 8.6 Hz).

Step 6. (5-{2-[(2′,3′,4′-Trimethoxy-biphenyl-3-carbonyl)-amino]-phenyl}-thiophen-2-yl)-acetic acid methyl ester (589 mg, 1.14 mmol) was dissolved in acetonitrile (10 mL) at rt and then treated with aq LiOH (5.7 mL of a 1 M solution, 5.7 mmol). The reaction mixture was stirred for 17 h at rt and then quenched by addition of 1 M aq HCl (pH ∼ 3), with cooling as necessary. The mixture was

extracted with EtOAc (three times), and the combined organic phases were washed with water and then brine, dried with Na_2SO_4, and then concentrated, to obtain (5-{2-[(2′,3′,4′-trimethoxy-biphenyl-3-carbonyl)-amino]-phenyl}-thiophen-2-yl)-acetic acid (586 mg of crude product, quant.) as a yellow solid. ^{1}H NMR (400 MHz, $CDCl_3$): 3.62 (s, 3 H); 3.87 (s, 2 H); 3.89 (s, 3 H); 3.92 (s, 3 H); 6.73 (d, 1 H, $J = 8.6$ Hz); 6.96-.99 (m, 1 H); 6.99 (d, 1 H, $J = 8.6$ Hz); 7.02 (d, 1 H, $J = 3.5$ Hz); 7.16 (td, 1 H, $J_1 = 7.6$ Hz, $J_2 = 1.0$ Hz); 7.36−7.43 (m, 2 H); 7.45 (t, 1 H, $J = 7.6$ Hz); 7.62 (d, 1 H, $J = 7.8$ Hz); 7.70 (d, 1 H, $J = 7.8$ Hz); 7.86 (s, 1 H); 8.37 (br. s, 1 H); 8.48 (d, 1 H, $J = 8.0$ Hz).

Step 7. (5-{2-[(2′,3′,4′-Trimethoxy-biphenyl-3-carbonyl)-amino]-phenyl}-thiophen-2-yl)-acetic acid (300 mg, 0.59 mmol) was dissolved in anhydrous dichloromethane (12 mL) at −78 °C under nitrogen, treated dropwise with a solution of BBr_3 in dichloromethane (3.6 mL of a 1 M solution, 3.6 mmol), stirred for additional 30 min at −78 °C, warmed slowly to rt, and stirred an additional 2 h at rt. The mixture was cooled to 0 °C, and then water was added dropwise, followed by dichloromethane with vigorous stirring. The reaction mixture was partitioned between water and EtOAc, and the aq phase was extracted with EtOAc (three times). The combined organic phases were washed with brine, dried with Na_2SO_4, and concentrated. The crude product was purified by preparative RP HPLC to obtain (5-{2-[(2′,3′,4′-trihydroxy-biphenyl-3-carbonyl)-amino]-phenyl}-thiophen-2-yl)-acetic acid (**56**, 110 mg, 40%) as a beige solid. ^{1}H NMR (400 MHz, CD_3OD): 3.86 (s, 2 H); 6.49 (d, 1 H, $J = 8.6$ Hz); 6.74 (d, 1 H, $J = 8.6$ Hz); 6.98 (d, 1 H, $J = 3.0$ Hz); 7.19 (d, 1 H, $J = 3.3$ Hz); 7.36 (t, 1 H, $J = 7.6$ Hz); 7.43 (t, 1 H, $J = 7.6$ Hz); 7.51 (t, 1 H, $J = 7.8$ Hz); 7.62 (d, 1 H, $J = 7.8$ Hz); 7.71−7.84 (m, 3 H); 8.08 (br. s, 1 H). MS (ESI) m/z 462.1 ($[M + H]^+$).

Biology. Static Molecular Binding Assay. The binding assay was performed with slight modifications as previously described.[36] In summary, 384-well Maxisorp plates (NUNC Roskilde/Denmark) were coated overnight in carbonate buffer pH 9.6 with goat anti human Fc mAB (10 μg/mL, Sigma, Steinheim, Germany). After being washed in assay buffer (25 mM HEPES, 150 mM NaCl, 1 mM $CaCl_2$ pH 7.4) and blocked (3% BSA in assay buffer), the plates were incubated for 2 h at 37 °C with human E-, P- or L-selectin/Fc-chimera (0.61 nM, R&D Systems, Wiesbaden, Germany). SLe^X-tyrosine sulfate polyacrylamide (Lectinity, Finland) carrying 15 mol % sLe^X, 10 mol % tyrosine sulfate, and 5 mol % biotin was complexed with Streptavidin-Peroxidase (Roche, Mannheim, Germany) in assay buffer without $CaCl_2$. This ligand complex (1:4500 in assay buffer), together with compounds in varying concentrations (assay buffer, 1%DMSO), was added to the wells precoated with E-, P-, or L-selectin/Fc-chimera. After incubation for 2 h at 37 °C, wells were washed six times with assay buffer incl. 0.005% TWEEN20 using a plate washer (BIO-TEK Instruments, Germany), developed for 10−15 min with TMB/H_2O_2 substrate solution (Boehringer Ingelheim, Mannheim, Germany), and stopped with 1 M H_2SO_4. Bound sLe^X−tyrosine sulfate ligand complex was determined by measuring optical density at 450 nm vs 620 nm in a Fusion α-FP reader (Packard Bioscience, Dreieich, Germany). Regressions and calculation of IC_{50} values were performed using a four-parameter logistic equation (Sigma Plot 8.0).

Dynamic HL-60 Cell Attachment Assay. Cell attachment under flow conditions was determined using a parallel flow chamber as published elsewhere.[22] In summary, polystyrene culture dishes (Corning, Wiesbaden, Germany) were coated with E- or P-selectin/Fc chimera (R&D Systems, Wiesbaden, Germany) and subsequently blocked with bovine serum albumin (Sigma, Steinheim, Germany). The dishes were fitted into the parallel flow chamber and mounted onto an inverted phase-contrast microscope (Olympus, Hamburg, Germany) equipped with a CCD camera (JVC) connected to a personal computer. Employing a peristaltic pump (Ismatec, Wertheim-Mondfeld, Germany), flow chamber experiments were performed in a recirculating configuration (without any visible pulsation) with a final concentration of 2.4 million HL-60 cells/mL (DSMZ, Braunschweig, Germany). The number of cells that attached to the substrate 5 min after continuous flow at a calculated flow shear of 1 dyn/cm^2 in the presence of 109 μM compound or vehicle alone (DMSO) was counted from five low power fields. Mean inhibition [% of vehicle control] was calculated from the mean cells/field of at least two independent experiments.

Acknowledgment. We thank Mrs. Sabine Sommer, Mrs. Petra Lindenberg, Mrs. Gabriele Dudda, and Mr. Frank Reinhardt for excellent technical support. In particular we would like to thank Dr. Brian Dupré, Encysive Pharmaceuticals Inc., Houston, TX, for in-depth reviewing this manuscript. This project is supported by grants of the ministry of economics of the State of Brandenburg and the European Union. Responsibility for the content of this publication rests upon the authors.

Supporting Information Available: Additional synthesis procedures and analytical data. This material is available free of charge via the Internet at http://pubs.acs.org.

References

(1) Weber, C. Novel Mechanistic Concepts for the Control of Leukocyte Transmigration: Specialization of Integrins, Chemokines, and Junctional Molecules. *J. Mol. Med.* **2003**, *81*, 4−19.

(2) Ley, K. The Role of Selectins in Inflammation and Disease. *Trends Mol. Med.* **2003**, *9*, 263−268.

(3) (a) Phillips, M. L.; Nudelman, E.; Gaeta, F. C. A.; Perez, M.; Singhal, A. K.; Hakomori, S. I.; Paulson, J. C. ELAM-1 Mediates Cell Adhesion by Recognition of a Carbohydrate Ligand, Sialyl- Le^X. *Science* **1990**, *250*, 1130−1132. (b) Walz, G.; Aruffo, A.; Kolanus, W.; Bevilacqua, M.; Seed, B. Recognition of ELAM-1 of the Sialyl-Le^X Determinant on Myeloid and Tumor Cells. *Science* **1990**, *250*, 1132−1135. (c) Berg, E. L.; Robinson, M. K.; Mansson, O.; Butcher, E. C.; Magnani, J. L. A Carbohydrate Domain Common to Both Sialyl Le^a and Sialyl Le^X is Recognized by the Endothelial Cell Leukocyte Adhesion Molecule ELAM-1. *J. Biol. Chem.* **1991**, *266*, 14869−14872. (d) Foxall, C.; Watson, S. R.; Dowbenko, D.; Fennie, C.; Lasky, L. A.; Kiso, M.; Hasegawa, A.; Asa, D.; Brandley, B. K. The Three Members of the Selectin Receptor Family Recognize a Common Carbohydrate Epitope, the Sialyl Lewis Oligosaccharide. *J. Cell Biol.* **1992**, *117*, 895−902.

(4) Zak, I.; Lewandowska, E.; Gnyp, W. Selectin Glycoprotein Ligands. *Acta Biochim. Pol.* **2000**, *47*, 393−412.

(5) (a) Kaila, N.; Thomas, IV, B. E.; Thakker, P.; Alvarez, J. C.; Camphausen, R. T.; Crommie, D. Design and Synthesis of Sialyl Lewis × Mimics as E-Selectin Inhibitors. *Bioorg. Med. Chem. Lett.* **2001**, *11*, 151−155. (b) Kaila, N.; Chen, L.; Thomas, IV, B. E.; Tsao, D.; Tam, S.; Bedard, P. W.; Camphausen, R. T.; Alvarez, J. C.; Ullas, G. β-C-Mannosides as Selectin Inhibitors. *J. Med. Chem.* **2002**, *45*, 1563−1566. (c) Hanessian, S.; Mascitti, V.; Rogel, O. Synthesis of Potent Antagonist of E-Selectin. *J. Org. Chem.* **2002**, *67*, 3346−3354. (d) Ikeda, T.; Kajimoto, T.; Kondo, H.; Wong, C. H. Design and Synthesis of An α-MannosylTerpenoid as Selective Inhibitor of P-Selectin. *Bioorg. Med. Chem. Lett.* **1997**, *7* (19), 2485−2490. (e) Hiruma, K.; Kajimoto, T.; Weitz-Schmidt, G.; Ollmann, I.; Wong, C. H. Rational Design and Synthesis of 1,1-Linked Disaccharide that is 5 Times as Active as Sialyl Lewis X in Binding to E-Selectin. *J. Am. Chem. Soc.* **1996**, *118*, 9265−9270. (f) Chervin, S. M.; Lowe, J. B.; Koreeda, M. Synthesis and Biological Evaluation of a New Sialyl Lewis X Mimetic Derived from Lactose. *J. Org. Chem.* **2002**, *67*, 5654−5662. (g) Höpfner, M.; Alban, S.; Schumacher, G.; Rothe, U.; Bendas, G. Selectin-Blocking Semisynthetic Sulfated Polysaccharides as Promising Anti-Inflammatory Agents. *J. Pharm. Pharmacol* **2003**, *55*, 1−10. (h) Rösch, M.; Herzner, H.; Dippold, W.; Wild, M.; Vestweber, D.; Kunz, H. Synthetische Inhibitoren der Zelladhäsion: Ein Glycopeptid aus dem E-Selektin-Liganden 1 (ESL-1) mit Arabino-Sialyl-Lewis^x-Struktur. *Angew. Chem.* **2001**, *113* (20), 3954−3956. (i) Ohmoto, H.; Nakamura, K.; Inoue, T.; Kondo, N.; Inoue, Y.; Yoshino, K.; Kondo, H. Studies on Selectin Blocker. 1. Structure-Activity Relationship of Sialyl Lewis X Analogs. *J. Med. Chem.* **1996**, *39*, 1339−1343. (j) Wada, Y.; Saito, T.; Matsuda, N.; Ohmoto, H.; Yoshino, K.; Ohashi, M.; Kondo, H. Studies on Selectin Blocker. 2. Novel Selectin Blocker as Potential Therapeutics for Inflammatory Disorders. *J. Med. Chem.* **1996**, *39*, 2055−2059. (k) Yoshino, K.; Ohmoto, H.; Kondo, N.; Tsujishita, H.; Hiramatsu, Y.; Inoue, Y.; Kondo, H. Studies on Selectin Blocker. 4. Structure − Function Relationship of Sulfated Sialyl Lewis X Hexasaccharide Ceramides towards E-, P-, and L- Selectin Binding. *J. Med. Chem.* **1997**, *40*, 455−462. (l) Baenteli, R.; Herold, P.; Bruns, C.; Patton, J. T.; Magnani, J. L.; Thoma, G. Potent E-Selectin Antagonists. *Helv. Chim. Acta.* **2000**, *83*, 2893−2907. (m) Thoma, G.; Magnani, J. L.;

Patton, J. T. Synthesis and Biological Evaluation of a Sialyl Lewis X Mimic with Significantly Improved E- Selectin Inhibition. *Bioorg. Med. Chem. Lett.* **2001**, *11*, 923−925. (n) Stahl, W.; Spengard, U.; Krezschmar, G.; Kunz, H. Synthesis of Deoxy Sialyl Lewis X Analogues, Potential Selectin Antagonists. *Angew. Chem., Int. Ed. Engl.* **1994**, *33*, 2096−2098. (o) Sprengard, U.; Kretzschmar, G.; Bartnik, E.; Hüls, C.; Kunz, H. Synthesis of an RGD-Sialyl-Lewis^x Glycoconjugate: A New Highly Active Ligand for P-Selectin. *Angew. Chem. Int. Ed. Engl.* **1995**, *34* (9), 990−993. (p) Sprengard, U.; Schudok, M.; Schmidt, W.; Kretzschmar, G.; Kunz, H. Multiple Sialyl Lewis^x N-Glycopeptides: Effective Ligands for E-Selectin. *Angew. Chem., Int. Ed. Engl.* **1996**, *35* (3), 321−324. (q) Tsukida, T.; Hiramatsu, Y.; Tsujishita, H.; Kiyoi, T.; Yoshida, M.; Kurokawa, K.; Moriyama, H.; Ohmoto, H.; Wade, Y.; Saito, T.; Kondo, H. Studies on Selectin Blockers. 5. Design, Synthesis, and Biological Profile of Sialyl Lewis X Mimetics Based on Modified Serine−Glutamic Acid Dipeptides. *J. Med. Chem.* **1997**, *40*, 3534−3541. (r) Hiramatsu, Y.; Moriyama, H.; Kiyoi, T.; Tsukida, T.; Inoue, Y.; Kondo, H. Studies on Selectin Blockers. 6. Discovery of Homologous Fucose Sugar Unit Necessary for E-Selectin Binding. *J. Med. Chem.* **1998**, *41*, 2302−2307. (s) Tsukida, T.; Moriyama, H.; Kurokawa, K.; Achiha, T.; Inoue, Y.; Kondo, H. Studies on Selectin Blockers. 7. Structure-Activity Relationships of Sialyl Lewis X Mimetics Based on Modified Ser-Gly Dipeptides. *J. Med. Chem.* **1998**, *41*, 4279−4287. (t) Martens, C. L.; Cwirla, S. E.; Lee R. Y. W.; Whitehorn, E.; Chen, E. Y. F.; Bakker, A.; Martin, E. L.; Wagstrom, C.; Gopalan, P.; Smith, C. W.; Tate, E.; Koller, K. J.; Schatz, P. J.; Dower, W. J.; Barrett, R. W. Peptides Which Bind to E-Selectin and Block Neutrophil Adhesion. *J. Biol. Chem.* **1995**, *270* (36), 21129−21136.

(6) (a) Spevak, W.; Foxall, C.; Charych, D. H.; Dasgupta, F.; Nagy, J. O. Carbohydrates in an Acidic Multivalent Assembly: Nanomolar P-Selectin Inhibitors. *J. Med. Chem.* **1996**, *39*, 1018−1020. (b) Pochechueva, T. V.; Ushakova, N. A.; Prebrazhenskaya, M. E.; Nifantiev, N. E.; Tsvetkov, Y. E.; Sablina, M. A.; Tuzikov, A. B.; Bird, M. I.; Rieben, R.; Bovin, N. V. P-Selectin Blocking Potency of Multimeric Tyrosine Sulfates In Vitro and In Vivo. *Bioorg. Med. Chem. Lett.* **2003**, *13*, 1709−1712. (c) John, A. E.; Lukacs, N. W.; Berlin, A. A.; Palecenda, A.; Bargatze, R. F.; Stoolman, L. M.; Nagy, J. O. Discovery of a Potent Nanoparticle P-Selectin Antagonist with Ant-Inflammatory Effects in Allergic Airway Disease. *FASEB* **2003**, *15*, 2296−2298. (d) Bruehl, R.; Dasgupta, F.; Katsumoto, T. R.; Tan, J. H.; Bertozzi, C. R.; Spevak, W.; Ahn, D. J.; Rosen, S. D.; Nagy, J. O. Polymerized Liposome Assemblies: Bifunctional Macromolecular Selectin Inhibitors Mimicking Physiological Selectin Ligands. *Biochemistry* **2001**, *40*, 5964−5974. (e) Thoma, G.; Duthaler, R. O.; Magnani, J. L.; Patton, J. T. Nanomolar E-Selectin Inhibitors: 700-Fold Potentiation of Affinity by Multivalent Ligand Presentation. *J. Med. Chem.* **2001**, *123*, 10113−10114. (f) Ushakova, N. A.; Prebrazhenskaya, M. E.; Bird, M. I.; Priest, R.; Semenov, A. V.; Mazurov, A. V.; Nifantiev, N. E.; Pochechueva, T. V.; Galanina, O. E.; Bovin, N. V. Monomeric and Multimeric Blockers of Selectins: Comparison of In Vitro and In Vivo Activity. *Biochemistry (Moscow*) **2005**, *70* (4), 432−439.

(7) (a) De Vleeschauwer, M.; Vaillancourt, M.; Goudreau, N.; Guindon, Y.; Gravel, D. Design and Synthesis of a New Sialyl Lewis X Mimetic: How Selective Are Selectin Receptors? *Bioorg. Med. Chem. Lett.* **2001**, *11*, 1109−1112. (b) Hiramatsu, Y.; Tsukida, T.; Nakai, Y. T.; Inoue, Y.; Kondo, H. Studies on Selectin Blocker. 8. Lead Discovery of a Non-Sugar Antagonist Using a 3-D Pharmacophore Model. *J. Med. Chem.* **2000**, *43*, 1476−1483. (c) Moriyama, H.; Hiramatsu, Y.; Kiyoi, T.; Achiha, T.; Inoue, Y.; Kondo, H. Studies on Selectin Blocker. 9. SARs of Non-Sugar Selectin Blocker against E-, P-, L-Selectin Bindings. *Bioorg. Med. Chem.* **2001**, *9*, 1479−1491. (d) Kaila, N.; Xu, G. Y.; Camphausen, R. T.; Xiang, Y. Identification and Structural Determination of A Potent P-Selectin Inhibitor. *Bioorg. Med. Chem.* **2001**, *9*, 801−806. (e) Slee, D. H.; Romano, S. J.; Yu, J.; Nguyen, T. N.; John, J. K.; Raheja, N. K.; Axe, F. U.; Jones, T. K.; Ripka, W. C. Devleopment of Potent Non-Carbohydrate Imidazole-Based Small Molecule Selectin Inhibitors with Antiinflammatory Activity. *J. Med. Chem.* **2001**, *44*, 2094−2107.

(8) Appeldoorn, C. C. M.; Bonnefoy, A.; Lutters, B. C. H.; Daenens, K.; van Berkel, T. J. C.; Hoylaerts, M. F.; Biessen, E. A. L. Gallic Acid Antagonizes P-Selectin-Mediated Platelet-Leukocyte Interactions. *Circulation* **2005**, *111* (1), 106−112.

(9) Kaila, N.; Somers, W. S.; Thomas, B. E.; Thakker, P.; Janz, K.; DeBernardo, S.; Tam, S.; Moore, W. J.; Yang, R.; Wrona, W.; Bedard, P. W.; Crommie, D.; Magnani, J. L.; Camphausen, R. T. Quinic Acid Derivatives as Sialyl Lewis^x-Mimicking Selectin Inhibitors: Design, Synthesis, and Crystal Structure in Complex with E-Selectin. *J. Med. Chem.* **2005**, *48*, 4346−4357.

(10) Romano, S. J. Selectin Antagonists: Therapeutic Potential in Asthma and COPD. *Treat. Respir. Med.* **2005**, *4* (2), 85−94.

(11) (a) Magnani, J. L. The Discovery, Biology, and Drug Development of Sialyl Le^a and Sialyl Le^X. *Arch. Biochem. Biophys.* **2004**, *426*, 122−131. (b) Chhabra, S. R. Recent Progress in the Design of Selectin Inhibitors. *Mini Rev. Med. Chem.* **2003**, *3*, 685−693. (c) Kaila, N.; Thomas, B. E. Design and Synthesis of Sialyl Lewis^X Mimics as E-and P-Selectin Inhibitors. *Med. Res. Rev.* **2002**, *22* (6), 566−601. (d) Simanek, E. E.; McGarvey, J.; Jablonowski, J. A.; Wong, C. H. Selectin-Carbohydrate Interactions: From Natural Ligands to Designed Mimics. *Chem. Rev.* **1998**, *98*, 833−862. (e) Bendas, G. Inhibitors of Membrane Receptors Involved with Leukocyte Extravasation. *Mini-Rev. Med. Chem.* **2005**, *5*, 575−584. (f) Romano, S. J.; Slee, D. H. Targeting Selectins for the Treatment of Respiratory Diseases. *Curr. Opin. Invest. Drugs* **2001**, *2*, 907−913. (g) Kaila, N.; Thomas, B. E. Selectin Inhibitors. *Expert Opin. Ther. Pat.* **2003**, *13*, 305−317.

(12) Schön, M. P. Inhibitors of Selectin Function in the Treatment of Inflammatory Skin Disorders. *Ther. Clin. Risk Manage.* **2005**, *1* (3), 201−208.

(13) (a) Collins, R. G.; Jung, U.; Ramirez, M.; Bullard, D. C.; Hicks, M. J.; Smith, C. W.; Ley, K.; Beaudet, A. L. Dermal and Pulmonary Inflammatory Disease in E- Selectin and P-Selectin Double-Null Mice is Reduced in Triple-Selectin-Null Mice. *Blood* **2001**, *98*, 727−735. (b) Jung, U.; Ley, K. Mice Lacking Two or All Three Selectins Demonstrate Overlapping and Distinct Functions for Each Selectin. *J. Immunol.* **1999**, *162*, 6755−6762. (c) Labow, M. A.; Norton, C. R.; Rumberger, J. M.; Lombard-Gillooly, K. M.; Shuster, D. J.; Hubbard, J.; Bertko, R.; Knaack, P. A.; Terry, R. W.; Harbison, M. L. Characterization of E-Selectin-Deficient Mice: Demonstration of Overlapping Function of the Endothelial Selectins. *Immunity* **1994**, *1*, 709−720.

(14) Poppe, L.; Brown, G. S.; Philo, J. S.; Nikrad, P. V.; Shah, B. H. Conformation of sLe^X Tetrasaccharide, Free in Solution and Bound to E-, P-, and L-Selectin. *J. Am. Chem. Soc.* **1997**, *119*, 1727−1736.

(15) Hicks, A. E. R.; Leppänen, A.; Cummings, R. D.; McEver, R. P.; Hellewell, P. G.; Norman, K. E. Glucosulfopeptides Modeled on P-Selectin Glycoprotein Ligand 1 Inhibit P-Selectin-Dependent Leukocyte Rolling In Vivo. *FASEB J.* **2002**, *16*, 1461−1462.

(16) Varki, A. Selectin Ligands: Will the Real Ones Please Stand Up? *J. Clin. Invest.* **1997**, *99*, 158−162.

(17) Cummings, R. D. Structure and Function of the Selectin Ligand PSGL-1. *Braz. J. Med. Biol. Res.* **1999**, *32*, 519−528.

(18) Graves, B. J.; Crowther, R. L.; Chandran, C.; Rumberger, J. M.; Li, S.; Huang, K.-S.; Presky, D. H.; Familletti, P. C.; Wolitzky, B. A.; Burns, D. K. Insight into E-Selectin/Ligand Interaction from the Crystal Structure and Mutagenesis of the lec/EGF Domains. *Nature* **1994**, *367*, 532−538.

(19) Somers, W. S.; Tang, J.; Shaw, G. D.; Camphausen, R. T. Insights into the Molecular Basis of Leukocyte Tethering and Rolling Revealed by Structures of P-and E-Selectin Bound to sLe^x and PSGL-1. *Cell* **2000**, *103* (3), 467−479.

(20) MOE 2004.03, Chemical Compouting Group Inc. (http://www.chemcomp.com).

(21) (a) Meyer, M.; Jilma, B.; Zahlten, R.; Wolff, G. Physicochemical Properties, Safety and Pharmacokinetics of Bimosiamose Disodium after Intravenous Administration. *Int. J. Clin. Pharmacol. Ther.* **2005**, *43*, 463−471. (b) Beeh, K. M.; Beier, J.; Meyer, M.; Buhl, R.; Zahlten, R.; Wolff, G. Bimosiamose, in Inhaled Small-Molecule Pan-Selectin Antagonist, Attenuates Late Asthmatic Reactions Following Allergen Challenge in Mild Asthmatics: A Randomized, Double-Blind, Placebo-Controlled Clinical Cross-Over-Trial. *Pulm. Pharmacol. Ther.* **2006**, *19*, 233−241. (c) Meyer, M; Beeh, K. M. Beier, J.; Beyer, D.; Aydt, E.; Zahlten, R.; Jilma, B.; Wolff, G. Tolerability and pharmacokinetics of inhaled bimosiamose disodium in healthy males. *Br. J. Clin. Pharmacol.* Published online Sep 20, 2006.

(22) Friedrich, M.; Bock, D.; Philipp, S.; Ludwig, N.; Sabat, R.; Wolk, K.; Schroeter-Maas, S.; Aydt, E.; Kang, S.; Dam, T. N.; Zahlter, R.; Sterry, W.; Wolff, G. Pan-Selectin Antagonism Improves Psoriasis Manifestation in Mice and Man. *Arch. Dermatol. Res.* **2006**, *297*, 345−351.

(23) Kogan, T. P.; Dupré, B.; Bui, H.; McAbee, K. L.; Kassir, J. M.; Scott, I. L.; Hu, X.; Vanderslice, P.; Beck, P. J.; Dixon, R. A. F. Novel Synthetic Inhibitors of Selectin-Mediated Cell Adhesion: Synthesis of 1,6-Bis[3-(3-carboxymethylphenyl)-4-(2-α-D-mannopyranosyl)phenyl]hexane (TBC1269). *J. Med. Chem.* **1998**, *41*, 1099−1111.

(24) Aydt, E. M.; Wolff, G. Development of Synthetic Pan-Selectin Anatgonists: A New Treatment Strategy for Chronic Inflammation in Asthma. *Pathobiology* **2002**−**03**, *70*, 297−301.

(25) Thoma, G.; Schwarzenbach, F. Simplified Sialyl Lewis^X Analogues with Improved E- Selectin Inhibition. *Helv. Chim. Acta* **2003**, *86*, 855−864.

(26) Kogan, T. P.; Dupré, B.; Keller, K. M.; Scott, I. L.; Bui, H.; Market, R. V.; Beck, P. J.; Voytus, J. A.; Revelle, B. M.; Scott, D. Rational Design and Synthesis of Small Molecule, Non-oligosaccharide Selectin Inhibitors: (α-D-Mannopyranosyloxy)biphenyl-Substituted Carboxylic Acids. *J. Med. Chem.* **1995**, *38*, 4976−4984.
(27) Schuster, M. C.; Mann, D. A.; Buchholz, T. J.; Johnson, K. M.; Thomas, W. D.; Kiessling, L. L. Parallel Synthesis of Glycomimetic Libraries: Targeting a C-Type Lectin. *Org. Lett.* **2003**, *5* (9), 1407−1410.
(28) Lin, C. C.; Shieh, D. E. The Anti-Inflammatory Activity of Scutellaria Rivularis Extracs and its Active Components, Baicalin, Baicalein and Wogonin. *Am. J. Chin. Med.* **1996**, *24*, 31−36.
(29) Chen, C. C.; Chow, M. P.; Huang, W. C.; Lin, Y. C.; Chang, Y. J. Flavonoids Inhibit Tumor Necrosis Factor-Alpha-Induced Up-Regulation of Intercellular Adhesion Molecule-1 (ICAM-1) in Respiratory Epithelial Cells Through Activator Protein-1 and Nuclear Factor-kappaB: Structure-Activity Relationships. *Mol. Pharmacol.* **2004**, *66* (3), 683−693.
(30) Middleton, E.; Kandaswami, C.; Theoharides, T. C. The Effect of Plant Flavonoids on Mammalian Cells: Implications for Inflammation, Heart Disease, and Cancer. *Pharmacol. Rev.* **2000**, *52* (4), 673−751.
(31) Anderson, M. B.; Levy, D. E.; Tang, P. C.; Musser, J. H.;Rao, N. Sialyl Lewis^X Mimetics Containing Flavanoid Backbones. International Patent WO97/31007, 1997.
(32) Dimitroff, C. J.; Lee, J. Y.; Schor, K. S.; Sandmaier, B. M.; Sackstein, R. Differential L-Selectin Binding Activities of Human Hematopoietic Cell L-Selectin Ligands, HCELL and PSGL-1. *J. Biol. Chem.* **2001**, *276*, 47623−47631.
(33) Kumamoto, M.; Sonda, T.; Nagayama, K.; Tabata, M. Effects of pH and Metal Ions on Antioxidative Activities of Catechins. *Biosci. Biotechnol. Biochem.* **2001**, *65* (1), 126−132.
(34) (a) Ahmad, N.; Mukhtar, H. Green Tea Polyphenols and Cancer: Biologic Mechanisms and Practical Implications. *Nutr. Rev.* **1999**, *57* (3), 78−83. (b) Gehm, B. D.; McAndrews, J. M.; Chien, P. Y.; Jameson, J. L. Resveratrol, a Polyphenolic Compound Found in Grapes and Wine, is an Agonist for the Estrogen Receptor. *Proc. Natl. Acad. Sci. U.S.A.* **1997**, *94*, 1438−14143. (c) Murakami, A.; Takahashi, D.; Hagihara, K.; Koshimizu, K.; Ohigashi, H. Combinatorial Effects of Nonsteroidal Anti-Inflammatory Drugs and Food Constituents on Production of Prostaglandin E_2 and Tumor Necrosis Factor-α in RAW264.7 Murine Macrophages. *Biosci. Biotechnol. Biochem.* **2003**, *67* (5), 1056−1062. (d) Molnar, V.; Garai, J. Plant-Derived Anti-Inflammatory Compounds Affect MIF Tautomerase Activity. *Int. Immunopharmacol.* **2005**, *5*, 849−856. (e) Dore, S. Unique Properties of Polyphenol Stilbenes in the Brain: More than Direct Antioxidant Actions; Gene/Protein Regulatory Activity. *Neurosignals* **2005**, *14* (1−2), 61−70. (f) Lee, W.; Min, W. K.; Chun, S.; Lee, Y. W.; Park, H.; Lee, D. H.; Lee, Y. K.; Son, J. E. Longer-Term Effect of Green Tea Ingestion on Atherosclerotic Biological Markers in Smokers. *Clin. Biochem.* **2005**, *38*, 84−87.
(35) (a) Molenaar, T. J. M.; Appeldoorn, C. C. M.; de Haas, S. A. M.; Micron, I. N.; Bonnefoy, A.; Hoylaerts, M. F.; Pannekoek, H.; van Berkel, T. J. C.; Kuiper, J.; Biessen, E. A. L. Specific Inhibition of P-Selectin-Mediated Cell Adhesion by Phage Display-Derived Peptide Antagonists. *Blood* **2002**, *100* (10), 3570−3577. (b) Appeldoorn, C. C. M.; Molenaar, T. J. M.; Bonnefoy, A.; van Leeuwen, S. H.; Vandervoort, P. A. H.; Hoylaerts, M. F.; van Berkel, T. J. C.; Biessen, E. A. L. Rational Optimization of a Short Human P-Selectin Binding Peptide Leads to Nanomolar Affinity Antagonists. *J. Biol. Chem.* **2003**, *278* (12), 10201−10207.
(36) Weitz-Schmidt, G.; Stokmaier, D.; Scheel, G.; Nifant'ev, N.E.; Tuzikov, A. B.; Bovin, N.V. An E-Selectin Binding Assay Based on a Polyacrylamide-Type Glycoconjugate. *Anal. Biochem.* **1996**, *238* (2), 184−190.

JM060536G